Research Paper

Biological characteristics of aging in human acute myeloid leukemia cells: the possible importance of aldehyde dehydrogenase, the cytoskeleton and altered transcriptional regulation

Maria Hernandez-Valladares[1,2,*], Elise Aasebø[1,2,*], Frode Berven[2], Frode Selheim[2,3], Øystein Bruserud[1]

[1]Department of Clinical Science, University of Bergen, Bergen 5021, Norway
[2]The Proteomics Facility of the University of Bergen (PROBE), University of Bergen, Bergen 5009, Norway
[3]The Department of Biomedicine, University of Bergen, Bergen 5009, Norway
*Equal contribution

Correspondence to: Maria Hernandez-Valladares, Øystein Bruserud; **email:** maria.hernandez-valladares@uib.no, oystein.bruserud@uib.no
Keywords: acute myeloid leukenia, age, risk, ALDH2, cytogenetics
Received: September 4, 2020 **Accepted:** November 20, 2020 **Published:** December 20, 2020

ABSTRACT

Patients with acute myeloid leukemia (AML) have a median age of 65-70 years at diagnosis. Elderly patients have more chemoresistant disease, and this is partly due to decreased frequencies of favorable and increased frequencies of adverse genetic abnormalities. However, aging-dependent differences may also contribute. We therefore compared AML cell proteomic and phosphoproteomic profiles for (i) elderly low-risk and younger low-risk patients with favorable genetic abnormalities; and (ii) high-risk patients with adverse genetic abnormalities and a higher median age against all low-risk patients with lower median age. Elderly low-risk and younger low-risk patients showed mainly phosphoproteomic differences especially involving transcriptional regulators and cytoskeleton. When comparing high-risk and low-risk patients both proteomic and phosphoproteomic studies showed differences involving cytoskeleton and immunoregulation but also transcriptional regulation and cell division. The age-associated prognostic impact of cyclin-dependent kinases was dependent on the cellular context. The protein level of the adverse prognostic biomarker mitochondrial aldehyde dehydrogenase (ALDH2) showed a similar significant upregulation both in elderly low-risk and elderly high-risk patients. Our results suggest that molecular mechanisms associated with cellular aging influence chemoresistance of AML cells, and especially the cytoskeleton function may then influence cellular hallmarks of aging, e.g. mitosis, polarity, intracellular transport and adhesion.

INTRODUCTION

Acute myeloid leukemia (AML) is an aggressive malignancy characterized by accumulation of immature myeloid cells in the bone marrow [1, 2]. There are two main subsets of AML. The minority of patient with the acute promyelocytic leukemia (APL) variant are characterized by specific genetic abnormalities, accumulation of immature promyelocytic cells, a clinical picture including severe coagulopathy, specific treatment and relatively good prognosis even for elderly patients [3]. In contrast, the non-APL variants of the disease are usually characterized by accumulation of immature blast cells in the bone marrow, it is very heterogeneous with regard to genetic abnormalities and elderly patients often have a more chemoresistant disease and thereby an adverse prognosis compared with younger patients [4]. All patients in the present

study have non-APL disease (referred to as AML in our article).

The median age at the first time of AML diagnosis is 65-70 year [1]; the elderly patients with chemoresistant disease thus constitute a large subset of patients. The chemoresistance and thereby the adverse prognosis even when receiving the most intensive treatment is probably caused by several factors. First, favorable cytogenetic abnormalities are less frequent in elderly patients [1, 4]. Second, a relatively large subgroup of these patients have secondary AML (i.e. secondary to previous cytotoxic therapy or a less aggressive chronic hematological malignancy) that can be associated with an adverse prognosis [4], although the independent prognostic impact of this factor in elderly AML patients has recently been questioned [5]. Third, cytogenetic as well as molecular genetic abnormalities (e.g. DNA (cytosine-5)-methyltransferase 3A, *DNMT3A*, and polycomb group protein ASXL1, *ASXL1*, mutations) with adverse prognostic impact are also more frequent in elderly patients [1, 4, 6]. However, additional aging-dependent abnormalities are probably also important for the adverse prognosis of elderly patients. The hematopoietic stem cells in elderly differ from the stem cell in younger individuals with regard to accumulation of mutations and increased frequency of clonal hematopoiesis that seems to predispose to later AML [7]. Age-associated epigenetic changes have also been described [7], and age-associated changes in the bone marrow microenvironment may preferentially support the expansion of cells with preleukemic characteristics [8–12]. Finally, aging hematopoietic stem cells are also characterized by increased numbers of mitochondria, metabolic alterations with decreased autophagy, nuclear abnormalities with decreased levels of lamin (LMNA) in the nuclear envelope and altered cellular polarity with differences in the intracellular distribution of important biomolecules [13–20]. A previous mRNA microarray study suggested that aged AML cells differed in their expression of certain mediators such as RAS, tyrosine-protein kinase Src (SRC) and tumor necrosis factor (TNF) [21].

Taken together all the observations described above suggest that several mechanisms contribute to the chemoresistance of many elderly AML patients. These mechanisms include factors that have a generally accepted prognostic impact independent of age but with age-dependent differences in their frequency. However, additional biological factors that become more frequent with aging are probably also important, and these last observations have led to the hypothesis that aging contributes to leukemogenesis [7]. It is not known whether similar aging-associated characteristics also contribute to the chemoresistance of elderly patients.

To further elucidate possible molecular mechanisms that contributes to chemoresistance especially in elderly individuals we compared the liquid chromatography tandem mass spectrometry (LC-MS/MS)-generated proteomic and phophoproteomic profiles of AML cells derived from contrasting patient groups: (i) elderly low-risk (median age of 68 years) *vs* younger low-risk patients (median age of 47 years) with favorable genetic abnormalities; and (ii) high-risk patients (median age of 74 years) with adverse genetic abnormalities *vs* all the low-risk patients (median age of 64.5 years) [1]. Both these comparisons demonstrated high aldehyde dehydrogenase (ALDH2) levels, altered expression of cytoskeletal proteins and an altered transcriptional regulation in AML cells derived from elderly patients.

RESULTS

Patients included in the study

Based on the AML cell samples collected at the first time of diagnosis and the predefined genetic criteria we selected 18 low-risk patients with favorable genetic prognosis and 15 high-risk patients with adverse genetic prognosis (see Materials and Methods for group definitions; Tables 1, 2 and Supplementary Tables 1, 2). In our present context the terms high- and low-risk refer to the risk of having a chemoresistant relapse even after the most intensive antileukemic therapy. The two groups differed significantly with regard to age, cause of their leukemia and morphological signs of differentiation. Low-risk patients were generally younger, none of them had secondary AML and half of them had normal karyotype (Tables 1, 2). The frequency of patients with monocytic AML cell differentiation (i.e. FAB M4/5) was higher in the low-risk group. However, the expression of the CD34 stem cell marker did not differ significantly between the two groups. Most high-risk patients were older and had complex cytogenetic abnormalities (i.e. ≥3 abnormalities).

In order to study the impact of morphological signs of differentiation in patient groups that differed significantly with regard to age, we carried out proliferation assays with primary AML cells derived from an alternative cohort of consecutive patients in the presence of hematopoietic growth factors (Supplementary Analysis Tables 1, 2). Our results showed that the proliferative responsiveness of patients with or without morphological signs of differentiation and with age above or below 65 years did not differ significantly. Thus, based on this analysis that included consecutive patients, i.e. not only high-/low-risk karyotypes but also normal and intermediate risk karyotype, we could not find any evidence for a general association between proliferative capacity and patient age/AML cell differentiation.

Table 1. Characteristics of the AML patient cohort of this study.

	High-risk patient group	Low-risk patient group	*P* value
Number of patients	15	18	
Median age (range), years	74 (50-87)	64.5 (33-79)	0.005
Sex (males/females)	10/5	10/8	NS
Secondary AML cases	6	0	0.005
Chemotherapy predisposing to later AML	1	0	
Previous hematological disease	5	0	
Signs of differentiation			
FAB M4/M5 (monocytic differentiation)	3	11	0.039
CD34 expression	12	10	NS
Adverse genetic abnormalities			
Complex karyotype	10		
Monosomal karyotype	1		
del 5, del 12, -7	4		
Favorable genetic abnormalities			
inv16, t(16;16)		4	
t(8;21)		5	
Normal karyotype, *FLT3* WT or low ITD ratio, *NPM1*-INS		8	
Normal karyotype, *FLT3* WT, *NPM1* WT, *CEBPA* mutated		1	

FAB, French-American-British; WT, wild-type; ITD, internal tandem duplication; INS, a 4 bp-insertion/duplication; NS, not significant.

Table 2. Characteristics of the elderly low-risk and younger low-risk patient subgroups based on an age threshold of 65 years.

	Elderly low-risk patient group	Younger low-risk patient group	*P* value
Number of patients	9	9	
Median age (range), years	68 (66-79)	47 (33-64)	<0.0001
Sex (males/females)	3/6	7/2	NS
Signs of differentiation			
FAB M4/M5 (monocytic differentiation)	7	4	NS
CD34 expression	5	5	NS
Favorable genetic abnormalities			
inv16, t(16;16)	3	1	NS
t(8;21)	2	3	NS
Normal karyotype, *FLT3* WT or low ITD ratio, *NPM1*-INS	4	4	NS
Normal karyotype, *FLT3* WT, *NPM1* WT, *CEBPA* mutated	0	1	NS

FAB, French-American-British; WT, wild-type; ITD, internal tandem duplication; INS, a 4 bp-insertion/duplication; NS, not significant.

The 33 AML patient samples were used to perform MS-based proteomics and phosphoproteomics analyses as follows. Firstly, we have carried out an age-dependent analysis in low-risk patients and compared the proteomic and phosphoproteomic profiles between nine elderly low-risk and nine younger low-risk (see Materials and Methods for subgroup definitions). Secondly, we have investigated whether the identified age-dependent differences were also observed when comparing high-risk and all the low-risk patients that differed in age and cytogenetics-related prognosis.

Effects of aging on the AML cell proteome; a proteomic comparison between elderly and younger low-risk patients

We obtained the proteome profiles of AML cells derived from nine elderly low-risk and nine younger low-risk patients using our FASP-based workflow (Figure 1). We quantified 5966 proteins, of which 4369 had a quantitative value in at least five patients in each group (Figure 2A). The proteome profiles from the elderly low-risk and younger low-risk patients were compared using *t*-test based statistical analysis and resulted in a small set of only 29 differentially expressed proteins, with 18 of them being upregulated and 11 downregulated for the elderly low-risk patients (Figure 2A, Supplementary file 1, Supplementary Table 3 upper part, Supplementary Table 4). Gene ontology (GO) enrichment analyses showed that regulation of T cell mediated immunity (i.e. syntaxin-7, STX7, and galectin-10, CLC) and oxidoreductase activity (i.e. aspartyl/asparaginyl beta-hydroxylase, ASPH, and ribosomal oxygenase 2, RIOX2) were more abundant GO terms in elderly low-risk patients (Figure 2B, top plot). The proteins enriched in this group were primarily located in organelles such as mitochondria and endoplasmic reticulum. Kyoto Encyclopedia for Genes and Genomes (KEGG) pathways analysis demonstrated that the upregulated elderly low-risk proteome was enriched with histidine, ascorbate and aldarate metabolism pathways (i.e. mitochondrial aldehyde dehydrogenase, ALDH2). In contrast, proteins involved in tRNA aminoacylation for protein translation (e.g. mitochondrial tryptophan-tRNA ligase, WARS2, and mitochondrial methionine-tRNA ligase, MARS2) and 5'-3' exodeoxyribonuclease activity (e.g. aprataxin, APTX) were less plenteous in elderly low-risk patients (Figure 2B, bottom plot).

It can be seen from Supplementary Table 3 that a major part of the proteins with differential expression is involved in either transcriptional regulation (five proteins), protein homeostasis/modulation (10 proteins) or mitochondrial functions/metabolism (10 proteins). Altered epigenetic/transcriptional regulation is regarded as a characteristic feature of aging in hematopoietic stem cells [7, 22, 23] together with alterations in metabolism [24–26] and/or mitochondrial functions [27–30], protein homeostasis [13, 22] and DNA repair/genomic instability [7, 23, 31]. Thus, even though the comparative analysis of the proteome from elderly and younger low-risk AML patients showed only 29 differentially expressed proteins, most of these proteins are involved in the regulation of cellular processes that are known to be altered in aging cells. Among them, NUMB (protein numb homolog) is of particular interest because it is involved in the regulation of asymmetrical cell division [32] and altered cell polarity is a hallmark of aging [31].

The effect of aging on the AML cell phosphoproteome; a comparison of elderly and younger low-risk patients

We constructed a dataset comprising 14,574 identified phosphopeptides, from which 11,962 class I protein

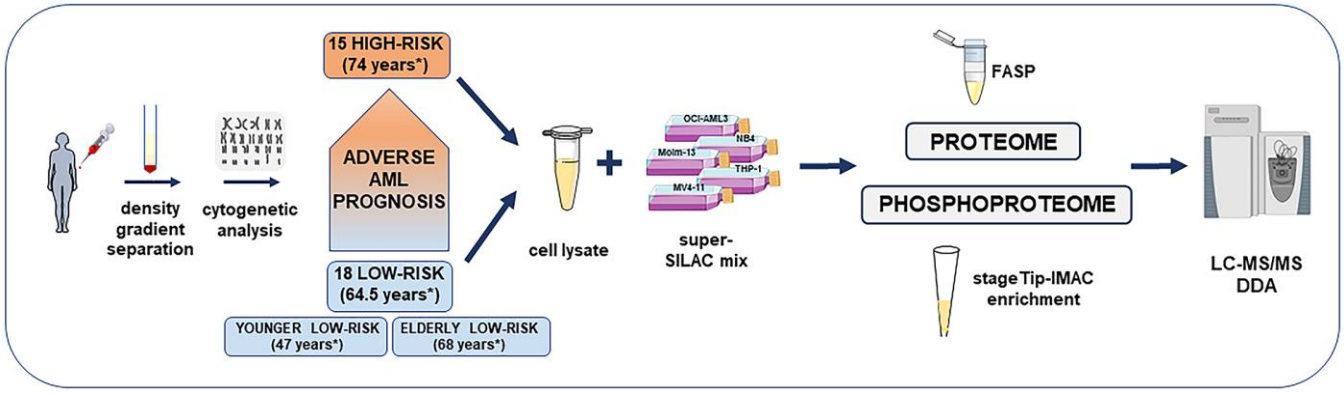

Figure 1. Overview of the high-risk and low-risk AML patient cohort and the liquid chromatography tandem mass spectrometry (LC-MS/MS) workflow for the proteome and phosphoproteome analysis. The study included AML cell samples from 15 high-risk and 18 low-risk patients collected at the time of first diagnosis. Patients were classified after cytogenetic and molecular genetic analyses. Low-risk patients were further split into elderly low-risk and younger low-risk patients. AML sample preparation steps for proteome and phosphoproteome analysis included AML cell enrichment by density gradient separation, genetic analyses with classification of patients, cell lysis, addition of the super-SILAC (stable isotope labeling with amino acids in cell culture) mix, filter-aided sample preparation (FASP)-based protein digestion and additional immobilized metal affinity chromatography (IMAC) enrichment of phosphopeptides before data-dependent acquisition (DDA) on the mass spectrometer. *Median age of each patient group or subgroup.

phosphorylation sites were quantified on 2818 proteins of nine elderly low-risk and nine younger low-risk patients. We identified 105 differentially regulated phosphorylation sites based on statistical analysis of 4767 phosphosites that could be quantified in at least five patients in each of these two groups (Figure 3A and Supplementary file 2). A cluster including 43 significantly upregulated and another cluster including 62 downregulated phosphosites in the elderly relative to the younger low-risk group were subjected to GO and KEGG pathways enrichment analysis (Supplementary Tables 3, 5, 6).

Regulation of filopodium assembly, vesicle cytoskeletal trafficking and RNA polymerase II transcription cofactor activity (Figure 3B, upper plot) represented GO terms with higher protein phosphorylation in elderly low-risk patients. These terms include phosphoproteins such as formin-binding protein 1-like (FNBP1L), protein kinase C-binding protein 1 (ZMYND8), Rho family-interacting cell polarization regulator 2 (FAM65B), dysbindin (DTNBP1), TP53-binding protein 1 (TP53BP1) and arginine-glutamic acid dipeptide repeats protein (RERE). The phosphoproteins enriched in elderly low-risk patients were primarily located in nuclear chromosomes, WASH complex, transverse tubules and endosome membranes. ARID1A (AT-rich interactive domain-containing protein 1A) may be of particular importance because this protein is a regulator of CDC42 (cell division control protein 42 homolog) which plays an essential role in the regulation

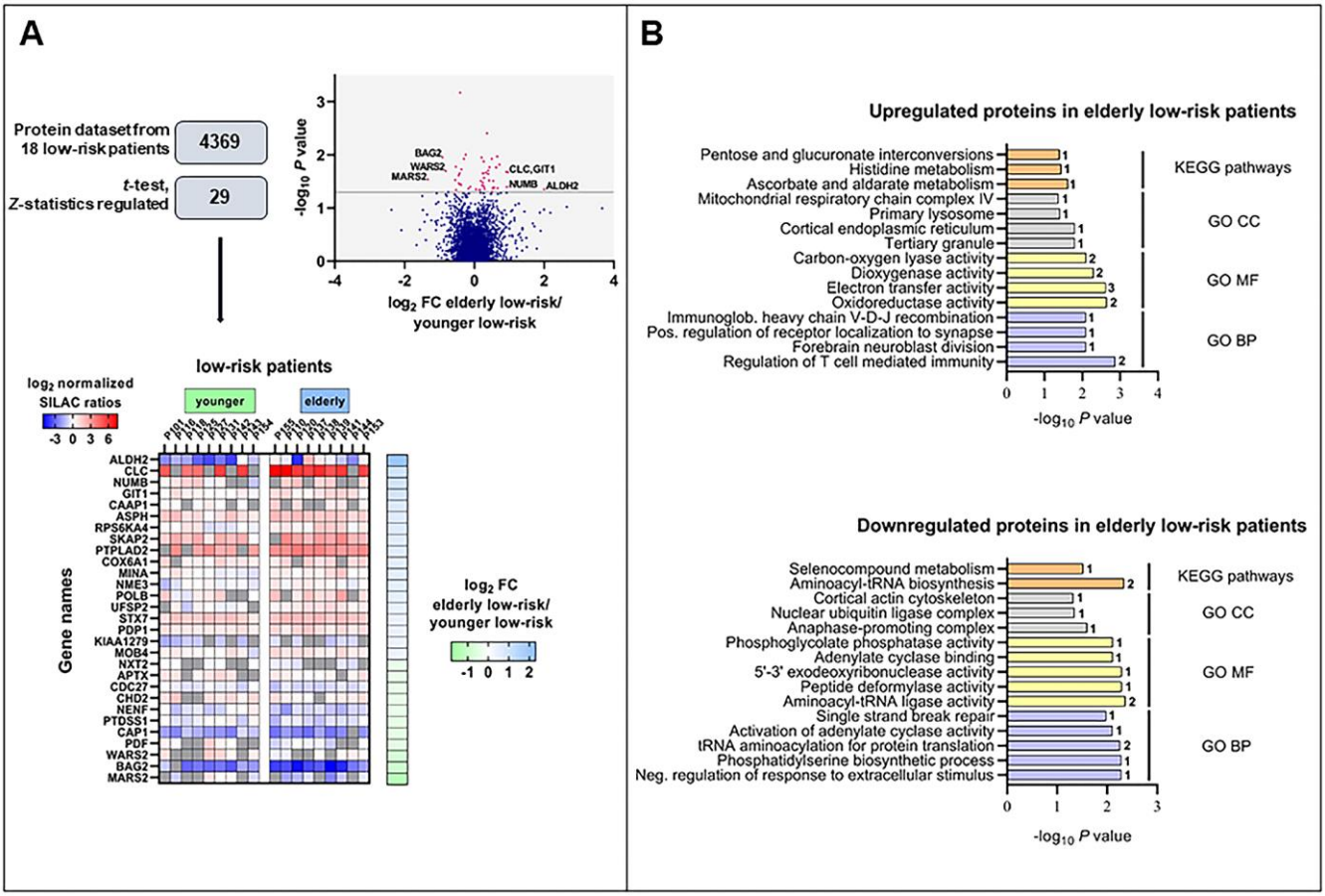

Figure 2. The regulated proteome in the study of elderly low-risk *vs* younger low-risk patients. (**A**) Overview of proteomic data analysis from elderly low-risk and younger low-risk patient samples. Volcano plot analysis of proteins quantified in at least five patients per group. Points (in magenta) above the non-axial horizontal grey line represent proteins with significantly different abundances (P <0.05). Heatmap of the 29 differentially expressed proteins in the elderly low-risk and younger low-risk groups. The $\log_2$ of fold change (FC) of protein levels in the elderly low-risk relative to the younger low-risk group is displayed on the right of the heatmap. (**B**) Gene Ontology (GO; BP, biological processes, with lilac bars; CC, cellular compartments, with light grey bars; MF, molecular functions, with yellow bars) and KEGG pathways (orange bars) analyses of upregulated and downregulated proteins in the elderly low-risk group. The various enriched GO terms and KEGG pathways are displayed on the y-axis while the corresponding $-\log_{10}$ P values are shown on the x-axis. The number of genes associated to a specific GO term or KEGG pathway is shown on the right side of the corresponding bar. Abbreviations were used in cases of long GO term (Immunoglob. for Immunoglobulin; Pos. for Positive and Neg. for Negative).

of actin and tubulin organization and thereby regulation of cellular polarity that can be lost in aging hematopoietic cells [13, 22]. KEGG pathways analysis showed similarities with the results from the GO term enrichment, i.e. the upregulated elderly low-risk phosphoproteome was enriched for protein export pathways. Several phosphoproteins involved in nitrogen compound metabolic process (e.g. histone-lysine N-methyltransferase 2A, KMT2A, and eukaryotic translation initiation factor 3 subunit F, EIF3F), regulation of cell cycle arrest (e.g. cyclin-dependent kinase 1 and 2, CDK1 and CDK2; nucleophosmin, NPM1) and transcriptional activator

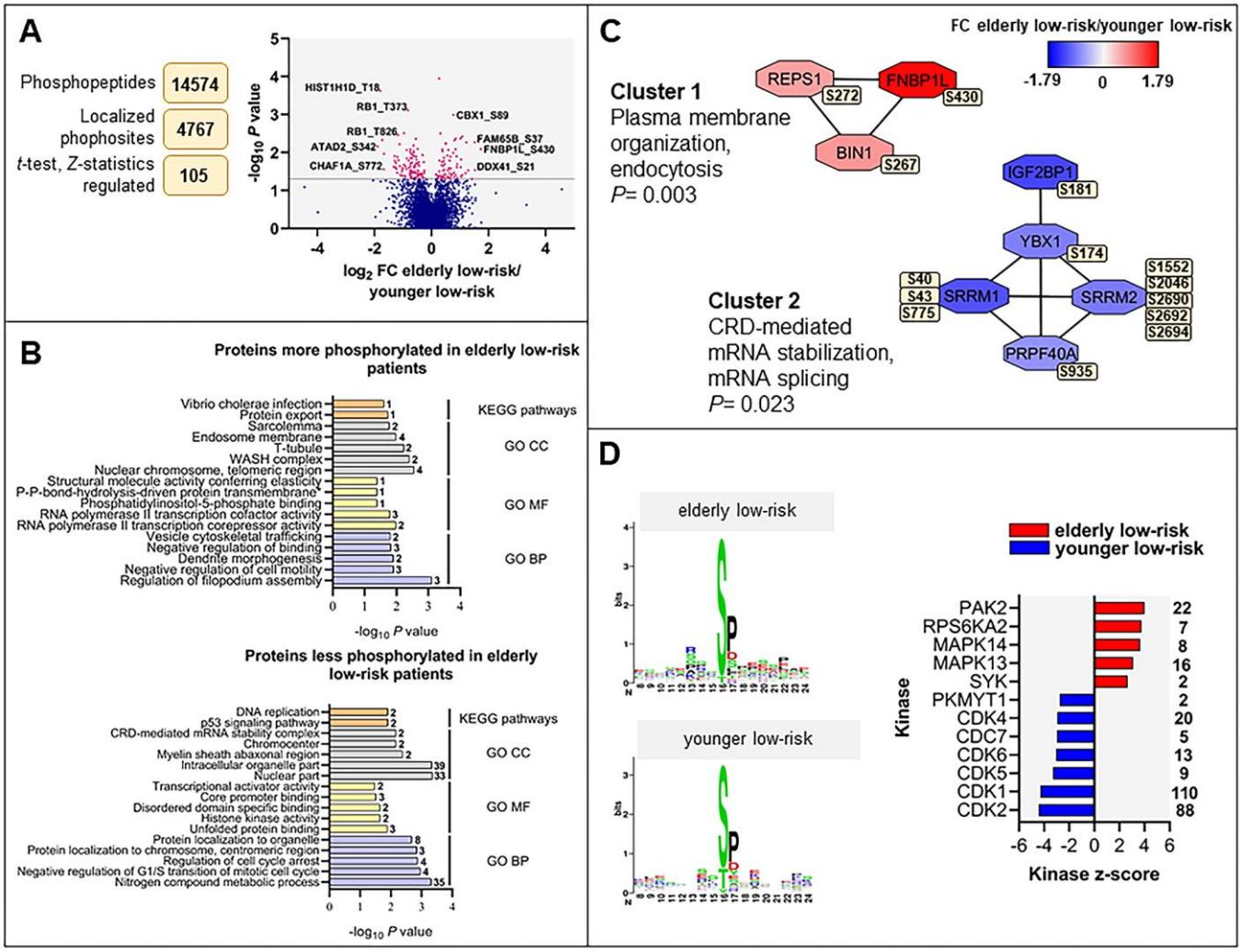

Figure 3. The regulated phosphoproteome in the study of elderly low-risk *vs* younger low-risk patients. (**A**) Overview of phosphoproteomic data analysis from elderly low-risk and younger low-risk patient samples. Volcano plot analysis of phosphosites quantified in at least five patients per group. Points (in magenta) above the non-axial horizontal grey line represent phosphosites with significantly different phosphorylation levels (P <0.05). (**B**) GO (BP terms with lilac bars; CC terms with light grey bars; MF terms with yellow bars) and KEGG pathways (orange bars) analyses of proteins with increased and decreased phosphorylation in elderly low-risk patients. The various enriched GO terms and KEGG pathways are displayed on the y-axis while the corresponding $-\log_{10}$ P values are shown on the x-axis. The number of genes associated to a specific GO term or KEGG pathway is shown on the right side of the corresponding bar. (**C**) Networks of protein-protein interactions (PPI) based on STRING database and visualized in Cytoscape after ClusterONE analysis. The significance of networks with high cohesiveness is shown with the P value of a one-sided Mann-Whitney U test. The differentially regulated phosphorylation sites are shown in yellow boxes next to each protein. FC of phosphorylation are color-coded; red-colored proteins showed a higher phosphorylation in elderly low-risk patients and blue-colored proteins showed a higher phosphorylation in the younger low-risk group. (**D**) Sequence motif analysis of the ± eight amino acids flanking the differentially regulated phosphorylation sites for each patient group and kinase-substrate enrichment analysis (KSEA) of differentially regulated and unregulated phosphorylation sites. The kinase z-score (x-axis) is the normalized score for each kinase (y-axis), weighted by the number of identified substrates indicated on the right side of the plot. Only significant predicted kinases with false discovery rate (FDR) values <0.05 were shown.

activity (e.g. ribosomal RNA processing protein 1 homolog B, RRP1B) were less phosphorylated in elderly low-risk patients (Figure 3B, bottom plot). Proteins less phosphorylated in this group showed a significant enrichment of DNA replication and p53 signaling KEGG pathways.

Several protein-protein interactions (PPI) networks of significant cohesiveness were found after ClusterONE analysis based on STRING interactions of differentially phosphorylated proteins (Figure 3C). The most significant network (cluster 1) consisted of three phosphoproteins with higher phosphorylation in elderly low-risk patients and being involved in plasma membrane organization and endocytosis (i.e. protein export found in the KEGG analysis). The second significant cluster involved mRNA stabilization and splicing proteins. Serine/arginine repetitive matrix protein 1 and 2 (SRRM1 and SRRM2) showed higher phosphorylation on multiple sites in younger low-risk relative to elderly low-risk patients. These splicing factors are phosphorylated on multiple serine and threonine residues by dual specificity tyrosine-phosphorylation-regulated kinase 3 (DYRK3) during the G2-to-M transition, after the nuclear-envelope breakdown [33] (i.e. regulation of transcription and cell cycle, see the KEGG analyses).

As shown in Supplementary Table 3, a majority of the total set of the differentially regulated phosphorylated sites were located in proteins involved in RNA synthesis/function (i.e. transcription factors, epigenetic regulation, histone modulation, RNA splicing and ribosomal regulation). Such altered transcriptional regulation is regarded as a hallmark of aging [31]; it is also a characteristic of hematopoietic stem cell aging [19, 20] and thus an important characteristic of AML in elderly patients [7].

Differences in AML cell kinase activity when comparing elderly low-risk and younger low-risk patients

To identify protein kinases differentially activated in elderly low-risk and younger low-risk patients we performed phosphorylation site motif analysis with the WebLogo tool [34] (Figure 3D, left plots). We found higher activity of several kinases such as protein kinase A and C (PRKACA, PRKCD; basophilic motif upstream to the differentially phosphorylated site), calmodulin-dependent protein kinase II (CaM kinase II; basophilic motif upstream to the differentially phosphorylated site), serine/threonine protein kinase PAK2 (basophilic motif upstream to the differentially phosphorylated site), casein kinase 2 (CSK2; acidic amino acid-based motif downstream to the differentially phosphorylated site) and extracellular signal-regulated kinases (ERK1/2; proline-directed motif downstream to the differentially phosphorylated site) in elderly low-risk patients. In contrast, cyclin-dependent kinases (CDKs; proline-directed motif downstream to the differentially phosphorylated site) substrates appeared more phosphorylated in the younger low-risk group.

The kinase-substrate enrichment analysis (KSEA) [35, 36], which is based on phosphorylation fold changes (FCs) to estimate kinase's activity, confirmed the higher activity of PAK2 and mitogen-activated protein kinases (MAPKs) in elderly low-risk patients and the higher activity of CDKs in the younger low-risk group (Figure 3D, right plot). KSEA analysis revealed a high number of CDK1 and CDK2 substrates from proteins such as ARID1A, LIG1 (DNA ligase 1), FOXK2 (forkhead box protein K2), NPM1 and retinoblastoma-associated protein (RB1).

We found five phosphosites in three different protein kinases in this data set using the activation loop analysis tool (see Materials and Methods). All of them (CDK1 T14, CDK2 T14, CDK1 Y15, CDK2 Y15 and GSG2 S147) can be phosphorylated during mitosis and were upregulated in younger low-risk relative to elderly low-risk patients.

Proteomic comparison of high-risk and all low-risk patients; different expression of neutrophil degranulation, platelet degranulation and cytoskeleton proteins

We compared the proteome profiles of AML cells derived from 15 high-risk and 18 low-risk patients. We quantified 6569 proteins, of which 5009 had a quantitative value in at least five patients in each group. The *t*-test based statistical analysis resulted in 205 differentially expressed proteins, 82 proteins were upregulated and 123 were downregulated in high-risk relative to low-risk patients (Supplementary Figure 1A and Supplementary file 3). Hierarchical clustering based on the 205 regulated proteins identified two main patient clusters (Figure 4A, left part), which corresponded to the high-risk and low-risk samples, although a distinct separation was not obtained. GO enrichment analysis showed that cytoskeleton organization, actin binding and integrin binding as biological process and molecular function GO terms were over-represented in high-risk patients (Figure 4A, right part). These terms include several tubulin (TUBB) chains, protein-tyrosine kinase 2-beta (PTK2B), cytoplasmic linker-associated protein 1 (CLASP1), actin-related protein 2/3 complex subunit 1A (ARPC1A), NCK-interacting protein with SH3 domain (NCKIPSD), TNF receptor-associated factor 2 (TRAF2) and NCK-interacting protein kinase (TNIK), alpha-

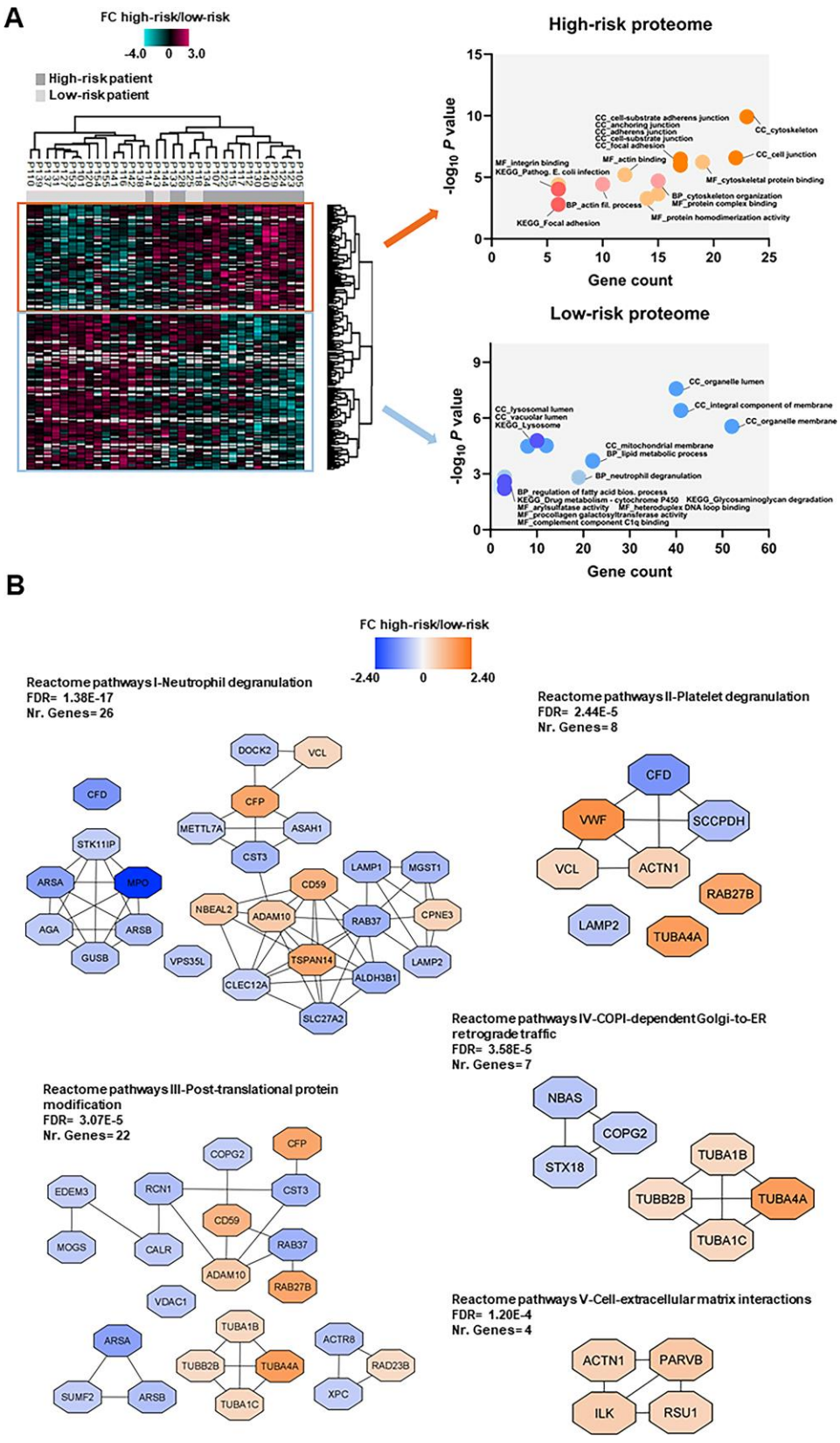

Figure 4. Proteomic differences between high-risk and low-risk patients; the importance of the cytoskeleton reflected in levels of neutrophil degranulation, platelet degranulation and endomembrane trafficking proteins. (**A**) Hierarchical clustering of 33 patients was based on the expression (SILAC $\log_2$ ratio) of 205 proteins with significantly different regulation in AML cells from high-risk (dark grey squares) and low-risk patients (light grey squares). Two vertical main clusters were observed, one dominated by proteins with

higher abundance in mostly high-risk patients (upper cluster) and the other by proteins with higher abundance in low-risk patients (lower cluster). GO and KEGG pathways analyses of the two protein clusters were performed to reveal enriched BP, CC and MF terms for the high-risk and low-risk patients. The various enriched GO terms and KEGG pathways are displayed in the scatter plot. The number of genes associated to a specific GO term or KEGG pathway (count) and the corresponding $-\log_{10}$ *P* values are shown on the x-axis and y-axis, respectively. Abbreviations were used in cases of long GO term or KEGG pathway name (Pathogen. for Pathogenic; fil. for filament). (**B**) Reactome term enrichment was performed using the STRING app (1.5.1) in Cytoscape. The five Reactome pathways with highest significance are shown with the corresponding FDR values. The protein nodes are colored according to their high-risk/low-risk FC, i.e. orange indicates increased abundance in the high-risk group and blue increased abundance in the low-risk group.

actinin-1 (ACTN1) and integrin-linked protein kinase (ILK). Moreover, KEGG pathways analysis confirmed that the focal adhesion and pathogenic *E. coli* infection pathways (i.e. several tubulin chains and actin-related protein 2/3 complex subunits) were enriched in the upregulated high-risk proteome.

In the low-risk proteome, proteins involved in neutrophil degranulation (i.e. extracellular secretion) and lipid metabolic processes such as complement factor D (CFD), myeloperoxidase (MPO), lysosome-associated membrane glycoprotein 1 and 2 (LAMP1/2), mitochondrial enoyl-CoA delta isomerase 1 (ECI1), 3-ketoacyl-CoA thilase, mitochondrial (ACAA2) and lysophosphatidylcholine acyltransferase 2 (LPCAT2) were higher expressed (Figure 4A, right part). Arylsulfatase and procollagen galactosyltransferase activities were the molecular functions more abundant in the low-risk group. As much as 43% of the proteins with higher abundance in low-risk patients were annotated to the organelle membrane in the cellular component analysis.

Analysis of Reactome terms showed that neutrophil degranulation (Reactome pathways I), platelet degranulation (Reactome pathways II) -both these granulation processes reflecting the extracellular secretion in myeloid cells-, post-translational protein modification (Reactome pathways III), COPI-dependent Golgi-to-ER retrograde traffic (Reactome pathways IV) and cell-extracellular matrix interactions (Reactome pathways V) pathways were enriched in the set of 205 regulated proteins (Figure 4B and Supplementary Table 7). We observed several clusters of upregulated proteins in the high-risk patient group in Reactome pathways III, IV and V including cytoskeleton proteins such as tubulin chains, ACTN1, ILK, beta-parvin (PARVB) and Ras suppressor protein 1 (RSU1). Clusters of upregulated proteins in the low-risk patient group were found in other Reactome pathways, such as the one comprised of arylsulfatase A (ARSA), arylsulfatase B (ARSB), MPO, N(4)-(beta-N-acetylglucosaminyl)-L-asparaginase (AGA), beta-glucuronidase (GUSB) and serine/threonine-protein kinase 11-interacting protein (STK11IP) in Reactome pathways I; ARSA, ARSB and inactive C-alpha-formylglycine-generating enzyme 2 (SUMF2) in Reactome pathways III; and syntaxin-18 (STX18), neuroblastoma-amplified sequence (NBAS) and coatomer subunit gamma-2 (COPG2) in Reactome pathways IV.

Few proteins in Reactome pathways I and II show an expression mainly or limited to myeloid cells, whereas a majority of them are expressed by various tissues/organs/cells and are important for membrane/organellar functions or protein metabolism/modulation. Thus, these networks seem to mainly reflect differences in fundamental and common cellular processes more than differences in the differentiation status of the cells.

Only ALDH2 had a similar differential expression both when comparing elderly low-risk *vs* younger low-risk and high-risk *vs* all low-risk patients

A main difference between our first comparison of elderly low-risk *vs* younger low-risk patients and this second comparison of high-risk *vs* all low-risk patients is the higher number of differentially expressed proteins in the latter analysis. Furthermore, only three proteins, ALDH2, Ufm1-specific protease 2 (UFSP2) and BAG family molecular chaperone regulator 2 (BAG2) were differentially regulated in both studies (Supplementary Figure 2A). Only ALDH2, a poor prognosis predictor in AML as well as in urothelial cancer ([37]; http://www.proteinatlas.org) showed a similar upregulation in both comparisons. Western blot analyses using lysates from nine high-risk and nine low-risk (five elderly low-risk and 4 younger low-risk) patient cells showed higher ALDH2 expression in high-risk and elderly low-risk when compared to all low-risk and younger low-risk patients, respectively (Supplementary Figure 3), although differences between groups were not statistically significant according to the Mann-Whitney test.

These observations are consistent with the hypothesis that ALDH2 expression reflects an adverse prognostic impact of age in AML.

Phosphoproteomic comparison of high-risk *vs* all low-risk patients; detection of differences in mitotic cell cycle regulation

We identified and quantified 14,990 class I protein phosphorylation sites from 3279 proteins when

comparing 15 high-risk and 18 low-risk patients. We found 239 differentially regulated phosphorylated sites based on statistical analysis of 6682 phosphosites, which were quantified in at least five patients in each group (Supplementary Figure 1B and Supplementary file 4). Hierarchical clustering using these 239 phosphosites clearly distinguished the phosphoproteome of the two patient groups (Figure 5A, left part). Two clusters, one containing 124 phosphosites and another with 115 phosphosites, were upregulated in the high-risk and in the low-risk patient group, respectively.

Cellular component GO analysis revealed an enrichment of upregulated cytoplasmic, cytoskeleton and membrane phosphoproteins for the high-risk patients, whereas organelle, organelle envelope and nuclear envelope structures were enriched in low-risk patients (Figure 5A, right part). While cell adhesion molecule binding, positive regulation intracellular signal transduction and small molecule metabolic process were the biological process and molecular function GO terms enriched in the high-risk group, positive regulation chromosome segregation, cell cycle checkpoint and Rho guanyl-nucleotide exchange factor activity were enriched in the low-risk patient group (Figure 5A, right part).

Reactome pathways for apoptotic execution phase and for mitotic prophase were found significantly enriched with proteins mainly of higher phosphorylation in the high-risk and in the low-risk patient group, respectively (Figure 5B and Supplementary Table 7). Two PPI networks of significant cohesiveness were found after ClusterONE analysis based on STRING interactions of differentially phosphorylated proteins (Figure 5C and Supplementary Table 7). The most significant network (cluster 2) consisted of six phosphoproteins involved in RNA processing and mRNA splicing, most of them with higher phosphorylation in low-risk patients. The other significant cluster included phosphoproteins of the mitotic cell cycle process (cluster 1). All phosphoproteins, except nuclear mitotic apparatus protein 1 (NUMA1), were significantly more phosphorylated in high-risk patients. A sequence logo analysis of the amino acids surrounding the phosphosites in cluster 1 suggested PRKACA and kinases of the PRKC family involved in the phosphorylation of the six cell cycle proteins (Supplementary Figure 4).

A final analysis of the regulated high-risk *vs* low-risk phosphosite set to study the interactions of their corresponding phosphoproteins in signal transduction with SIGNOR [38] (Figure 5D) confirmed the relevant roles of CDKs in the regulation of the cell cycle, RNA processing, translation and cytoskeleton function that are observed in AML patients with different risk-related cytogenetics abnormalities.

Several protein kinases are differentially activated in AML cells derived from high-risk and all low-risk patients

To identify protein kinases differentially activated in the two groups we performed phosphorylation site motif analysis with IceLogo [39]. We found a basophilic motif upstream to the differentially phosphorylated site in high-risk patients when compared to low-risk patients, suggesting an activation of PRKACA, PRKCA and PRKCD (Figure 6A). Furthermore, KSEA confirmed the higher activity of PRKACA and predicted several other serin/threonine protein kinases (PRKG1, PRKD1 and PRKCD), MAPKs and RAC-alpha serine/threonine protein kinase (AKT) isoforms activated in the high-risk patient group (Figure 6B). Although PRKACA and AKT1 phosphorylated a large number of substrates (52 and 51, respectively), CDK1 (significantly predicted with unadjusted P= 0.022 in the KSEA; therefore not displayed in Figure 6B which shows predicted kinases at FDR <0.05) phosphorylated 140 substrates in this group. Serine/threonine protein kinase MAK, which phosphorylates proteins involved in protein ubiquitation and in the transcriptional coactivation of androgen receptor, was activated in the low-risk patient group.

We found eight phosphosites on five different protein kinases in the data set of 239 differentially regulated phosphorylation sites. Three phosphosites on serine/threonine-protein kinase D2 (PRKD2; S197, S198 and S706; the latter located in the activation loop of the kinase), involved in the regulation of cell proliferation via ERK1/2 signaling, in Golgi membrane trafficking and cell adhesion, were significantly more phosphorylated in the high-risk patient group. PRKD2 S706 is probably phosphorylated by the members of the PRKC family [40]. SRC S17 and CDK1 Y15 were also significantly more phosphorylated in the high-risk patient group. Phosphorylation of CDK1 Y15 by Wee-1 like protein kinase 1/2 (WEE1/2) inhibits the protein kinase activity and acts as a negative regulator of entry into mitosis (G2 to M transition) whilst phosphorylation by PRKCD activates the G2-M DNA damage checkpoint after UV irradiation [41]. Dephosphorylation at CDK1 Y15 by active M-phase inducer phosphatase 1/2 (CDC25A/B) leads to CDK1 activation at the G2-M transition [42]. The higher phosphorylation of CDK1 (and CDK2) Y15, along with T14 phosphorylation, was further confirmed by a separate MS-based immune-affinity enrichment (Supplementary Table 8 and Supplementary file 5). The significantly higher phosphorylation of CDK1/2 T14 alone in high-risk patients was also observed in the latter analysis (not significant in the general phosphopeptide enrichment analysis with P= 0.078). Finally, tyrosine-protein kinase Fes/Fps (FES), a regulator of the actin

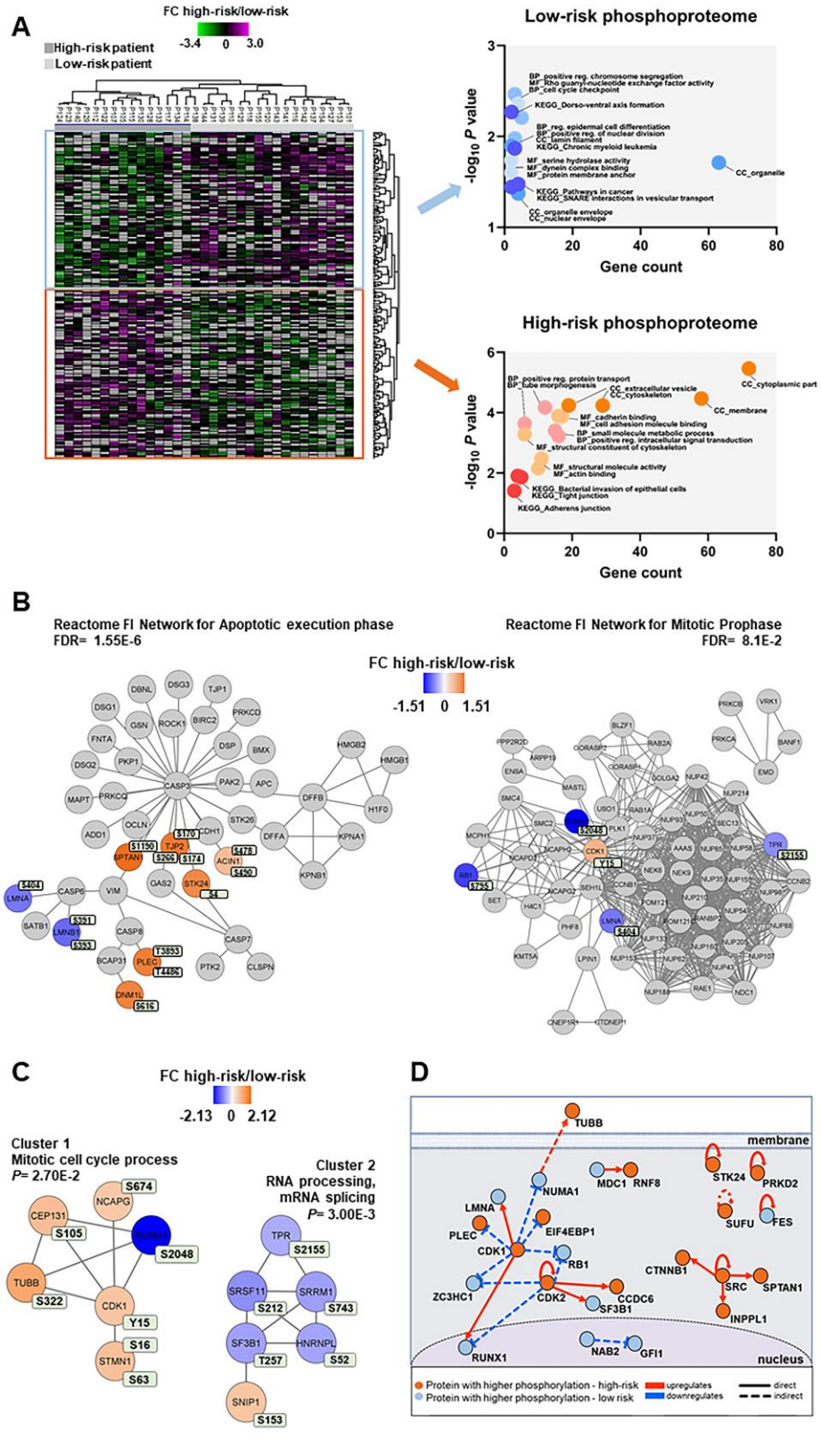

Figure 5. Phosphoproteomic differences between high-risk and low-risk patients; the importance of the cytoskeleton, mitotic cell cycle regulation and CDK activities. (**A**) Hierarchical clustering of the 33 patients based on the phosphorylation level (SILAC $\log_2$ ratio) of 239 phosphosites with significant differences between high-risk and low-risk patient samples. Two vertical main clusters were observed, one dominated by phosphosites with higher phosphorylation in low-risk patients (upper cluster) and the other

by phosphosites with higher phosphorylation in high-risk patients (lower cluster). GO and KEGG pathways analyses of the two corresponding phosphoprotein clusters were performed to reveal enriched BP, CC and MF terms in the high-risk and low-risk patient samples. The various enriched GO terms and KEGG pathways are displayed in the scatter plot. The number of genes associated to a specific GO term or KEGG pathways (count) and the corresponding $-\log_{10}$ *P* values are shown on the x-axis and y-axis, respectively. Abbreviations were used in cases of long GO term or KEGG pathway name (reg. for regulation). (**B**) Visualization of hit Reactome pathways was performed using the ReactomeFIViz app (7.2.3) in Cytoscape. Two significant Reactome networks (FDR <0.05) that mapped phosphoproteins with differential phosphorylation in our dataset are shown. The protein nodes are colored according to their high-risk *vs* low-risk $\log_2$ phosphorylation FC, i.e. orange indicates increased phosphorylation in the high-risk group and blue increased phosphorylation in the low-risk group. (**C**) Networks of PPI based on STRING database and visualized in Cytoscape after ClusterONE analysis. The significance of networks with high cohesiveness is shown with the *P* value of a one-sided Mann-Whitney U test. The differentially regulated phosphorylation sites are shown in light green boxes next to each protein. FC of phosphorylation are color-coded; orange-colored proteins showed a higher phosphorylation in the high-risk group and blue-colored proteins showed a higher phosphorylation in the low-risk group. (**D**) Causal relationships between phosphoproteins with differentially regulated phosphorylation sites in the high-risk *vs* low-risk phosphoproteome set was studied with SIGNOR. The analysis showed the pivotal role of CDKs in the control of cell cycle, cytoskeleton and translation phosphoproteins. Nodes and types of relationships are displayed as indicated on the bottom part of the design.

cytoskeleton and microtubule assembly, S408; and STK26 (serine/threonine-protein kinase 26), a mediator of cell growth, T327 and T328 were significantly more phosphorylated in the low-risk patient group.

The results from Western blotting did not show any significant difference in protein phosphorylation of several kinase candidates between the high-risk and the low-risk groups (Supplementary Figure 5). However, despite the different spectrum of sensitivity of both methods, the increased activity of CDK1, PRKCD and PRKACA in the high-risk group detected by the MS-based data was also observed in the Western blots (Supplementary Figure 5). We also noticed a distinct CDK1 T161-Y15 phosphorylation pattern for each of the patient groups. While these two phosphosites were similarly phosphorylated in low-risk patients, CDK1 T161 phosphorylation was different of that observed in CDK1 Y15 in high-risk patients suggesting a different CDK1 regulation for each of the groups. Moreover, the phosphorylation levels of PRKCD S645 and PRKACA T197 were parallel for each patient showing a joint activation of both kinases.

Only LSP1 had a similar differential phosphorylation both when comparing elderly low-risk *vs* younger low-risk and high-risk *vs* all low-risk patients

Five phosphosites on proteins lymphocyte-specific protein 1 (LSP1), lamina-associated polypeptide 2, isoform alpha (TMPO), CDK1, CDK2 and N-acetyltransferase ESCO2 (ESCO2) were quantified in both our comparisons, i.e. elderly low-risk *vs* younger low-risk and high-risk *vs* all low-risk patients (Supplementary Figure 2B). Only LSP1_S177, an actin-binding cytoskeleton protein involved in cell migration and possibly phosphorylated at that residue by MAPKAPK2 and/or protein kinase C [43], showed significant associations with high age/increased risk of relapse in both our comparisons. However, CDK1/2 Y15 showed increased phosphorylation in high-risk and in younger low-risk patients. These apparently conflicting observations on CDK's activity illustrate that the impact of certain age-associated proteomic differences may differ between patient subsets and depend on the biological/genetic context.

DISCUSSION

Elderly AML patients seem to have more chemoresistant disease than younger patients; this is at least partly due to a lower frequency of low-risk genetic abnormalities and a higher frequency of at least certain high-risk abnormalities in elderly patients [1, 6] although some high-risk abnormalities (e.g. MLL abnormalities) do not show such age-dependent differences [44].

Many elderly patients cannot receive intensive and potentially curative treatment due to an unacceptable risk of treatment-related mortality [1], and elderly patients receiving intensive treatment do not receive the same consolidation therapy as the younger patients, e.g. patients above 60 years of age cannot receive high-dose cytarabine [1]. A difference in the survival for younger and elderly AML patients may therefore reflect differences in chemotherapy and not (only) differences in chemosensitivity. However, younger and elderly AML patients often receive the same induction chemotherapy, and differences in the complete remission rate will therefore reflect differences in chemosensitivity that also are relevant for long-term survival [45]. Several observations suggest that elderly patients have a lower remission rate. First, the initial experience after introduction of the conventional "7+3" cytarabine/anthracycline induction regimen showed a long-term remission of 20-25% for younger and 10% for elderly patients [46]. Second, a large study of intensive treatment showed a significant decrease of complete remission rate with age; the rate was 65% for

patients below 56 years of age but only 33% for patients above 75 years [47]. Finally, several studies have investigated the remission rate of patients above 60 years of age receiving the conventional "7+3" regimen but with the increased daunorubicine dose of 60 mg/m^2/day.

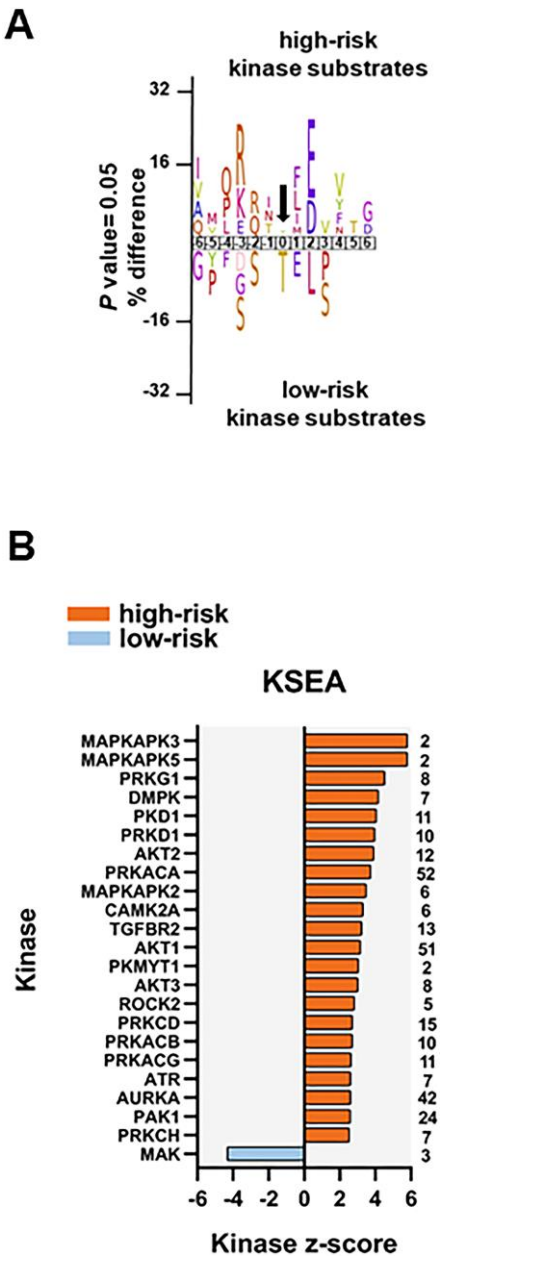

Figure 6. Kinase prediction analysis of the high-risk *vs* low-risk phosphoproteome. (**A**) Sequence motif analysis of the ± six amino acids flanking the differentially regulated phosphorylation sites for either group. (**B**) KSEA of differentially regulated and unregulated phosphorylation sites. The kinase z-score (x-axis) is the normalized score for each kinase (y-axis), weighted by the number of identified substrates indicated on the right side of the plot. Significant predicted kinases with FDR <0.05 are shown.

Complete remission rates corresponding to 33-51% of the patients have been observed for elderly patients [48, 49] whereas younger patients have shown remission rates exceeding 70% [50, 51] and this higher rate is expected because previous studies of younger patients have described remission rates corresponding to 60-85% [52]. Taken together these observations suggest that elderly AML patients have a more chemoresistant disease.

Normal hematopoietic stem cells develop biological signs of aging [12–20] and the aim of our study was therefore to investigate whether similar biological characteristics of aging could be detected at the proteomic and phosphoproteomic level in AML cells derived from elderly patients. To do so we only included patients with relatively high levels of circulating AML cells (i.e. peripheral blood leukemization) so that enriched cell populations could then be prepared by simple gradient separation alone [53, 54].

In the present study we wanted to compare patient subsets with regard to *in vivo* chemosensitivity (i.e. AML-free survival) and the association between leukemization and *in vivo* chemosensitivity is regarded as uncertain or weak compared with the impact of genetic abnormalities [45]. Several studies have suggested that a prognostic impact of leukemization is seen only when peripheral blood blast counts exceed 100 x 10^9/L [55–57]. Only a small minority of our patients had such high blood blast counts; therefore, the impact of those few patients on our present results is in our opinion limited.

Bone marrow samples were not used because the diagnostic criteria for AML is usually at least 20% blasts, but for patients with favorable cytogenetic abnormalities there is no such blast criteria [58]. More extensive cell separation procedures that may alter the biological characteristics of the leukemic cells [53] would have therefore been necessary if bone marrow samples had been used. Moreover, blood and bone marrow AML cells seem to have only minor differences [59], and even clonal heterogeneity as well as hierarchical organization of the AML cell clones can be demonstrated in peripheral blood AML cells [60, 61]. The use of cryopreserved biobank samples allowed us to carefully select patients according to our predefined cytogenetic criteria, and follow-up experiments of the same patients were also possible.

Our study should be regarded as population-based because we included all patients in a defined geographical area who were diagnosed with AML during a defined time period. For this reason, our study included a relatively large number of elderly patients,

and many elderly and unfit patients did not receive intensive and potentially curative antileukemic treatment [1]. Twelve out of 18 low-risk patients received intensive treatment, and this is expected from the age distribution of these patients. Only four of these 12 patients became long-term survivors. This is not unexpected as one patient was lost from follow-up, we had one early death due to hyperleukocytosis, three elderly patients died from toxicity during intensive consolidation therapy, one patient did not receive consolidation therapy due to severe toxicity and one allotransplanted patient died from Graft versus host disease. Taken together this explains why we have a relatively low long-term AML free survival even for patients with low-risk disease who received intensive chemotherapy.

A relatively high non-relapse mortality is expected for elderly patients [1], and this was also seen in our present study. Our patients were selected according to cytogenetic criteria, and when taking into account that the median age of patients with first diagnosis of AML is 65-70 years [1] it is expected that relatively few of our patients received intensive and potentially curative therapy because of their age. Due to this heterogeneity of our patients with regard to antileukemic treatment, extensive survival analyses were not possible.

Our high- and low-risk cell populations showed additional differences respecting patient age, frequency of secondary AML and morphological signs of differentiation. These differences are expected because favorable cytogenetic abnormalities are most common in younger patients [1, 6, 58]; AML secondary to previous chemotherapy or chronic myeloid malignancies (i.e. chronic myeloproliferative neoplasia, myelodysplastic syndrome) is most common for elderly patients [5, 62]; and both favorable cytogenetic abnormalities as well as *NPM1* mutations are associated with morphological signs of differentiation [58, 63, 64]. High age is associated with adverse prognosis, and to further investigate age-dependent factors independent of the genetic abnormalities we firstly investigated a group of patients with a limited number of well-defined genetic abnormalities (karyotype; receptor-type tyrosine-protein kinase *FLT3*, *FLT3*, *NPM1* and CCAAT/enhancer-binding protein alpha, *CEBPA*, mutations) generally accepted to be associated with a good prognosis [1]. Thus, we compared elderly and younger patients with a favorable prognosis based on analyses of these cytogenetic abnormalities (i.e. the elderly low-risk and the younger low-risk patient groups with median age of 68 and 47 years, respectively). This scientific strategy was chosen because we assumed that an additional age-dependent adverse prognostic impact may be easier to detect for patients with favorable prognosis than for patients with an already adverse prognosis due to their cytogenetic abnormalities. This approach is supported by a recent publication describing an independent adverse prognostic impact of secondary AML only for younger patients [5].

In the second analysis of this study we compared a group with adverse prognosis (i.e. the high-risk patient group with a higher median age of 74 years) *vs* a group with favorable prognosis (the whole low-risk patient group with a lower median age of 64.5 years) to investigate whether possible proteomic or phosphoproteomic characteristics identified in the first comparison could still be detected when comparing high-risk and low-risk patients. Our MS-based methodology is reliable and reproducible for this kind of studies as we have shown by validation with alternative non MS-based technologies in two previous papers [65, 66].

Among the hallmarks of aging, including hematopoietic stem cell aging, are altered cellular communication, altered intracellular trafficking/polarity influencing the communication with neighboring cells/stroma, detoxification/stress responses, and altered transcriptional regulation due to various different mechanisms including altered epigenetic regulation [23, 31]. The most important age-associated differences described in our present studies are increased ALDH2 levels (stress responses), cytoskeletal modulation (trafficking/mitosis/transport/polarity) and transcriptional regulation. These main differences can all be relevant for aging and may then be involved in leukemogenesis and chemosensitivity for elderly AML patients.

Aldehyde dehydrogenase (ALDH) proteins are intracellular enzymes that oxidize cellular aldehydes and thereby participate in regulation of differentiation and development of chemoresistance [67]. Both our primary AML cell comparisons suggested that the protein levels of ALDH2 are increased in elderly AML patients; this was true both when comparing elderly low-risk and younger low-risk patients, and high-risk *vs* all low-risk patients. Both experimental and clinical studies suggest that ALDH2 activity is important for leukemogenesis and/or chemosensitivity in AML. First, ALDH2 activity and *ALDH2* gene polymorphisms seem to be involved in carcinogenesis for various malignancies [68]. This seems to be true not only for solid tumors but also for leukemogenesis; the involvement of ALDH (including ALDH2) for progression of preleukemic Fanconi anemia to bone marrow failure/AML is suggested both by animal models and clinical studies [69–72]. Second, ALDH2 can influence the signaling through several intracellular pathways involved in regulation of apoptosis, and it can thereby have antiapoptotic effects [73]. ALDH inhibition has a synthetically lethal effect in

AML cells when combined with glutathione peroxidase-4 inhibition [74], and it can overcome both bortezomib and cytarabine resistance in Down syndrome-associated AML [75]. High ALDH2 activity is also associated with resistance to doxorubicin [76], the drug that is combined with cytarabine in conventional AML induction chemotherapy [1]. Third, ALDH activity can be detected in primary human AML cells, but the activity differs between patients and also between cells within the same hierarchically organized AML cell populations [77]. Patients with a generally high ALDH activity in their AML cells show decreased survival [77]. There is an association between high ALDH activity and high-risk karyotype [78] and high ALDH activity in AML cells is associated with an increased risk of relapse for patients with the favorable t(8;21) abnormality [79]. A recent study even suggested that ALDH2 expression could be included in a 4-gene expression prognostic signature for patients with intermediate-risk AML [80]. Finally, ALDH activity is detected both in normal hematopoietic and leukemic stem cells, but the activity in these two cell types seems to differ [81]. This may explain the observations from previous studies describing that ALDH inhibition can eradicate leukemic stem cells but at the same time spares normal hematopoietic stem cells [73, 78]. Taken together these observations suggest that ALDH activity/ALDH2 expression is important for chemosensitivity in human AML, and our present study suggests that this impact is associated with aging.

Our comparison of patient cohorts also identified several cytoskeletal proteins that were associated with differences in age. The cytoskeleton is important for intracellular trafficking and exocytosis/endocytosis, mitosis, for the cellular contact with neighboring cells and the extracellular matrix [82, 83]. Firstly, cytoskeletal proteins differed both in their expression level and in their phosphorylation when comparing elderly low-risk and younger low-risk patients (Figure 3B, 3C; Supplementary Tables 3–6). Second, differences in cytoskeletal proteins were also detected when comparing high-risk *vs* all low-risk patients (Figures 4B, 5B and Supplementary Table 7), especially those ones involved in membrane trafficking, post-translational protein modification and extracellular matrix interactions. Cytoskeleton proteins can be altered as a part of the aging process [84, 85] and the associations between age and altered levels/phosphorylation of cytoskeletal proteins may therefore reflect an impact of aging in AML. Finally, it should be emphasized that ALDH2 is a cytoskeleton-interacting protein [86] and cytoskeletal proteins were also included in the various interacting molecular networks identified in our studies.

It can be seen from Supplementary Table 1 and Table 1 that morphological signs of monocytic differentiation is more common for younger patients with low-risk disease. This difference is expected because both favorable cytogenetic abnormalities as well as *NPM1* insertions are associated with myeloid differentiation [58, 63, 64]. Furthermore, the data presented in Figure 4 showed that high- and low-risk patients also differ with regard to proteins involved in neutrophil and platelet degranulation. The question is therefore whether the other observed proteomic or phosphoproteomic differences (e.g. organellar functions, regulation of proliferation/mitosis) observed in our study reflect differences in differentiation rather than chemosensitivity, but in our opinion associations with differentiation seem less likely. Important characteristics of the identified proteins belonging to the neutrophil and platelet degranulation networks (Figure 4B) are summarized in Supplementary Table 7. Most of these proteins are expressed in a wide range of cells/tissues and not only in myeloid cell subsets; an observation suggesting that these proteins are important for cellular functions with regard to organellar functions/intracellular trafficking and not only for myeloid cell subsets (i.e. not specific signs of myeloid differentiation). Furthermore, we investigated the *in vitro* proliferative responsiveness of primary AML cells derived from an external cohort of consecutive patients. Even though we observed an expected and statistically significant association between young age and monocytic differentiation for this cohort, neither *in vitro* proliferative responsiveness nor expression of stem cell/molecular differentiation markers showed any significant associations with morphological AML cell differentiation (Supplementary Analysis Tables 1, 2). Taken together these observations therefore suggest that the organellar/degranulation/mitosis networks identified in Figures 4B, 5B, 5C represented aging-dependent rather than differentiation-dependent differences between AML cells.

Both the proteomic and phosphoproteomic analyses suggested that mitotic regulation differs between elderly/high-risk and younger/low-risk patients. When analyzing the proliferative AML cell capacity for a group of consecutive patients we did not find any evidence for a general association between proliferative capacity and differentiation of the AML cells (Supplementary Analysis Table 2). These observations support the hypothesis that the observed differences in regulation of mitosis/proliferation are not caused by differences in AML cell differentiation. Previous clinical studies also support the hypothesis that regulation of proliferation/mitosis is important for chemosensitivity of primary human AML cells. First, autonomous *in vitro* proliferation detected with a 6 days [^{3}H]-thymidine incorporation assay similar to our present suspension culture assay (Supplementary Analysis Table 2) was associated with an adverse

prognosis in a clinical study including AML patients below 60 years of age and receiving intensive chemotherapy [87]. The same was observed in another study using a 7 days colony formation assay [88] and in a study of cytokine-dependent proliferation [89]. Third, growth of leukemic cells after subcutaneous inoculation in immunodeficient mice is also associated with poor clinical outcome [90] and the same is true for primary human AML cells capable of long-term *in vitro* proliferation in suspension cultures prepared in cytokine-supplemented medium alone without stromal cell support [60]. Even though most of these observations were made for young AML patients, they illustrated that differences in the regulation of AML cell proliferation were associated with differences in prognosis/chemosensitivity, and the differences in molecular regulators of proliferation/mitosis detected in our present study may therefore reflect age-dependent contributions to a molecular profile that is important for the regulation of both mitosis/proliferation and clinical chemosensitivity.

Targeting of the cytoskeleton is regarded as a possible therapeutic strategy in human AML, and several Aurora kinase inhibitors are now in clinical trials for various malignancies [91, 92]. However, despite these clinical studies very few previous investigations have focused on the cytoskeleton in primary AML cells [93–95]. To the best of our knowledge the present study is the first to give a broad and detailed characterization of the cytoskeleton in primary AML cells including a description of patient heterogeneity and possible associations with chemoresistance and/or aging. Our present observations suggesting that the cytoskeletal function is important for chemosensitivity are further supported by a recent study where the development of chemoresistant AML relapse after intensive chemotherapy was associated with altered expression and/or phosphorylation of cytoskeletal proteins [66].

Transcriptional networks are altered in AML patients by several mechanisms that include transcription factor dysregulation by mutation or by translocation or downstream of signaling pathways [96]. We observed higher levels of several transcription repressors (e.g. RERE and ZMYND8) and lower phosphorylation of mRNA stabilization/splicing proteins (e.g. SRRM1/2) in elderly low-risk patients (Figure 3B, 3C). A lower phosphorylation of the same and different RNA processing proteins was also detected (e.g. SRRM1 and serine/arginine-rich splicing factor 11, SRSF11) in high-risk patients when they were compared to all low-risk patients (Figure 5C). Several transcriptional networks of different AML subtypes have been recently described as well as their required role for tumor maintenance and targeting of these altered networks might offer new therapeutic approaches to eliminate the subsistence program of AML cells [97].

Our phosphoproteomics analysis showed that the CDK family appeared to be more activated in younger low-risk patients, especially CDK1 and CDK2 with 110 and 88 substrate counts, respectively, according to the KSEA (Figure 3D). Among these substrates we identified FOXK2 and RB1. FOXK2 is hyperphosphorylated during mitosis by CDK1 and, to a lower extent, CDK2 [98]. The underphosphorylated, active form of RB1 interacts with transcription factor E2F1 (E2F1) and represses its transcription activity, leading to cell cycle arrest [99]. As RB1 was more phosphorylated in younger low-risk patients, E2F1 might be more active and induce myeloid cell-cycle progression [100]. Thus, our results suggest a tight control of the cell-cycle progression in younger low-risk patients.

Our studies also suggest that other biological characteristics of the leukemic cells also differ between elderly low-risk and younger low-risk patients. This includes molecules of the p53 signaling pathway (Figure 3B), which can also be altered as a part of the aging process [101–103]. G2 and S phase-expressed protein 1 (GTSE1), a protein that regulates microtubules (MT) stability during mitosis by inhibiting the mitotic centromere-associated kinesin (MCAK) MT depolymerase activity [104], appeared more phosphorylated in younger low-risk patients.

The regulated phosphoproteome of high-risk patients was involved in apoptotic execution, mitotic prophase, cell cycle progress and RNA processing (Figure 5B–5D). The higher phosphorylation of CDK1 and CDK2 at T14 and Y15, identified by general phosphoenrichment and phosphotyrosine immunoaffinity enrichment, and the higher number of CDK1 substrates identified by KSEA revealed a pivotal performance of these kinases in high-risk patients. Among these substrates, we identified NUMA1, a MT-binding protein that plays a role in the formation and maintenance of the spindle poles and the alignment and the segregation of chromosomes during mitotic cell division [105]. Phosphorylation and dephosphorylation of this protein determine its enrichment at the cell cortex and its association with the dynein-dynactin complex.

The phosphoproteomic analysis of both comparisons of the present study shows that CDKs seem to be activated in both younger low-risk and high-risk patients and target different substrates that might influence prognosis in AML. Moreover, the phosphorylation of CDK1/2 T161 and Y15 active sites was more heterogeneous among high-risk than among low-risk patients (Supplementary Figure 5). We have previously shown

that CDKs were also more activated at the time of first diagnosis for patients that relapsed within a 5-year follow-up after intensive and potentially curative therapy [65]. Taking together, CDKs play determinant roles in AML prognosis and relapse, and the prognostic impact seems to differ between patient subsets and depends on the genetic/biological context.

CONCLUSIONS

Our comparison of elderly low-risk and younger low-risk AML patients suggest that ALDH2 levels, cytoskeletal modulation and altered transcriptional regulation are consistent with an effect of aging on leukemogenesis and chemosensitivity in human AML. The role of kinases such as CDKs on age and disease seems to depend on the biological context and to differ between patient subsets. Elderly patients with high-risk AML seem to differ from all younger patients with low-risk disease with regard to the same cellular processes, even though the molecular mechanisms differ, and few other single molecules (e.g. LSP1) were identified in the two comparisons. Thus, our study suggests age-dependent alterations contributes to chemoresistance in human AML.

MATERIALS AND METHODS

Selection of patients and preparation of patient cells

All cell samples in the present study were derived at the first time of diagnosis before start of any antileukemic treatment. Our institution is responsible for diagnosis and treatment of patients with AML in a defined geographical area, and the patients included in our present study represent all patients from this area during a defined time period that fulfilled defined criteria established before start of the study. First, to ensure a high quality of the analyzed samples with at least 95% AML cells we included only patients with high levels of peripheral blood AML cells, i.e. at least 10 x 10^9 total leukocytes and at least 80% of these circulating leukocytes being leukemic cells. Second, among these consecutive patients with high levels of circulating AML cells, we selected all patients who fulfilled predefined genetic criteria for adverse and favorable prognosis as can been seen from Supplementary Table 1. These criteria are based on the European Leukemia Net (ELN) guidelines [1]. The ELN classification of AML is based on karyotyping together with molecular-genetic analyses, and patients are classified as having favorable, intermediate or adverse prognosis. This risk stratification does not take into account other pretreatment risk factors like peripheral blood blast count at the time of diagnosis, previous hematological malignancy (i.e. myelodysplastic syndrome, chronic myelomonocytic leukemia or chronic myeloproliferative neoplasia) and previous exposure to cytotoxic therapy for other diseases [1]. The classification does not take into account response to first induction cycle and minimal residual disease (MRD) after remission induction either [1, 45, 106, 107].

The patients with adverse prognosis included ten patients with complex karyotype and five patients with either monosomal karyotype, del 5 or -7. These adverse prognosis patients represent all patients who fulfilled the cytogenetic criteria for high-risk disease. Patients were screened for *FLT3* and *NPM1* mutations but additional mutational analyses for identification of additional adverse prognosis patients were not available during the defined time period, and for this reason these adverse prognosis patients were selected based on cytogenetic criteria alone. These patients will be referred to as high-risk patients. The median age of this patient group is 74 years.

The patients with favorable prognosis included all patients with the cytogenetic abnormalities inv(16), t(16;16) and t(8;21). We also included all patients with normal karyotype, wild-type *FLT3* and *NPM1* insertion as well as one patient with normal karyotype, low ratio of internal tandem duplication mutation of *FLT3*, *FLT3*-ITD, and *NPM1* insertion (Supplementary Table 1, patient F17) and another patient with *CEBPA* mutation (Supplementary Table 1, patient F18). Analysis of the *FLT3*-ITD ratio was not available as a routine analysis during this time period and only one patient could be classified as favorable based on these criteria (Supplementary Table 1). These patients will be referred to as low-risk patients. The median age of this patient group is 64.5 years.

More characteristics of the high-risk and low-risk patient groups are summarized in Tables 1, 2, and more detailed comparisons are presented in Supplementary Tables 1, 2. All patients were Caucasians.

As we included patients with high levels of circulating AML blasts at the time of first diagnosis, we could prepare highly enriched AML cell populations (>95% purity) by a standardized method based on density gradient separation alone (for a detailed discussion see references [53, 54, 65]). All samples were cryopreserved by using the same standardized method. The patient samples included in our study did not differ significantly with regard to peripheral blood blast count or storage time in liquid nitrogen.

Patient grouping for MS-based proteomic and phosphoproteomic analysis

In order to compare patient groups with different cytogenetics-based prognosis, we selected 15 high-risk

and 18 low-risk patients for subsequent proteomics analyses. The difference of the median age between the two groups was statistically significant (P= 0.005, Table 1). In order to study the influence of age in low-risk patients, we further divided the 18 patients in two subgroups of nine patients each, according to an age threshold of 65 years at the time of diagnosis, i.e. the elderly low-risk (median age of 68 years) and the younger low-risk (median age of 47 years). This threshold was chosen because it corresponds to the median age of patients at the first diagnosis of AML and it has also been used to distinguish between young/middle aged and elderly patients (i.e. not fit for the most intensive chemotherapy) in previous clinical studies [1, 108, 109]. The difference of the median age between the two subgroups was statistically significant (P <0.0001). This and other patient characteristics of the low-risk subgroups are shown in Table 2.

Peptide preparation

Our standard sample preparation of patient cell lysate in 4% sodium dodecyl sulfate (SDS)/0.1 M Tris-HCl (pH 7.6), the filter-aided sample preparation (FASP) procedure with AML patient samples and the immobilized metal affinity chromatography (IMAC) for phosphopeptide enrichment have been described previously [65, 110]. In short, 20 µg of each patient lysate was mixed with 10 µg of an AML-specific super-SILAC mix [111] for proteomic analyses, and digested according to the standard FASP protocol [110, 112]. The super-SILAC spiked peptide samples were fractionated using styrenedivinylbenzene-reversed phase sulfonate (SDB-RPS) plugs (Empore Discs, 3M) for proteome analysis [113]. The phosphoproteomics samples (226-2506 µg) were mixed with the super-SILAC mix at 1:2 ratio (w:w; super-SILAC mix:AML patient sample), FASP processed and enriched using the IMAC procedure. Extra labeled peptides samples (600-1479 µg) were also FASP prepared for phosphotyrosine immunoprecipitation (IP). IP was performed using PTMScan pTyr antibody beads (p-Tyr-1000; Cell Signaling Technology) according to the manufacturer's protocol. All the peptides samples were brought to equal volumes of binding buffer before antibody incubation. Eluted Tyr-phosphopeptides were cleaned up with 3-C18-disks-stage tips before MS analysis.

LC-MS/MS measurements

Peptide sample preparation prior to proteome and phosphoproteome analysis and settings of the LC-MS/MS runs on a Q Exactive HF Orbitrap mass spectrometer coupled to an Ultimate 3000 Rapid Separation LC system (Thermo Scientific) were carried out as described earlier [65]. Tyr-phosphopeptides were pre-concentrated on a 2 cm × 75 µm ID Acclaim PepMap 100 trapping column and separated on a 25 cm × 75 µm ID EASY-spray PepMap RSLC analytical column (Thermo Scientific). The Tyr-phosphopeptides were eluted during a 105 min binary gradient with solvent A (0.1% formic acid) and solvent B (0.1% formic acid/acetonitrile). The gradient started at 5% B from 0–5 min and increased to 7% B from 5–5.5 min, then to 22% B from 5.5–65 min, to 35% B from 65–87 min, and to 90% B from 87–92 min. Hold at 90% from 92-102 min, then ramped to 5% B from 102–105 min. The Q Exactive HF mass spectrometer was operated in data dependent acquisition (DDA) mode. Full MS scans (scan range 375–1500 m/z) were acquired in profile mode with a resolution R = 60 000 using an AGC target value of 3×10^6 charges. MS/MS scans were acquired in profile mode for the top 10 precursors. The AGC target value was set to 1×10^5 charges with a maximum injection time of 110 ms and a resolution R = 60 000. The normalized collision energy was 28 and the isolation window was 1.2 m/z with null m/z offset. The dynamic exclusion lasted for 20s.

The super-SILAC proteomic, phosphoproteomic and Tyr-phosphoproteomic samples were analyzed as three separate experiments in a controlled randomized order (i.e. samples from each patient group were distributed equally over the analysis sequence) with a LC-MS quality control (HeLa protein digest) run approximately every 10 patient samples.

Data analysis

LC-MS/MS raw files were processed with MaxQuant software version 1.5.2.8 [114, 115]. The spectra were searched against the concatenated forward and reversed-decoy Swiss-Prot Homo sapiens database version 2018_02 using the Andromeda search engine [116]. The Perseus 1.6.1.1 platform was used to analyze and visualize protein groups and phosphosites [117]. MaxQuant-normalized SILAC ratios were inverted, $\log_2$ transformed and normalized again using width adjustment. Hierarchical clustering of significantly differential proteins and phosphosites was done with Perseus using the Pearson correlation function and complete linkage. Volcano plots were done with Prism8 (GraphPad). GO and KEGG pathways analysis was performed using a GO tool [118]. The most significantly over-represented GO and KEGG pathways terms with P <0.05 were displayed in bar or scatter plots in Prism8. The amino acid distribution surrounding the phosphosites was analyzed using iceLogo (P= 0.05) with the sequence windows obtained in the MaxQuant-generated phosphosite output file [39]. Sequence logo analyses

from a small number of phosphopeptide sequences were generated with WebLogo [34]. Kinase activity estimates were inferred by the KSEA App. [35, 36]. Regulated and unregulated phosphosites were analyzed with the PhosphoSitePlus [119] and NetworKin [120] databases using a substrate count and a NetworKin score cutoff of 5. Kinase activation loop analysis was performed with the tools for phosphoproteomics data analysis at http://phomics.jensenlab.org. PPI networks were obtained by using the STRING database version 11.0 with interactions derived from experiments and databases at a high confidence score of 0.7 [121]. Networks were visualized using the Cytoscape platform version 3.3.0 [122]. The ClusterONE plugin was used to identify protein groups of high cohesiveness [123]. Reactome term enrichment and visualization of hit pathways were performed using the STRING app (1.5.1) [124] and the ReactomeFIViz app (7.2.3) [125, 126], respectively. Causal relationships between phosphoproteins were studied with the SIGnaling Network Open Resource (SIGNOR) 2.0 [38]. Venn diagrams were made with Biovenn [127].

Western blotting

Western blotting from nine high-risk and nine low-risk patient cells were performed. Twenty µg of each SDS-based cell lysate was loaded on a NuPAGE 4-12% Bis-Tris protein gel (ThemoFisher Scientific) and transferred onto a nitrocellulose membrane (Amersham Protran, GE Healthcare Life Sciences) in an XCell II Blot Module (ThermoFisher Scientific). Antibodies were purchased from Cell Signaling Technology and Abcam. They were used according to manufacturer's guidelines. Chemiluminescence was developed with SuperSignal West kits (Thermo Scientific) and measured on a LAS-3000 imager (Fujifilm). Band intensities for each protein were determined by densitometry software Image J [128]. Band intensities of a protein spotted at approximately 62 kDa on Ponceau-stained membranes were used for normalization.

Statistical analysis

Proteins and phosphosites (localization probability >0.75) with at least five individual SILAC ratios in each patient group were selected for two-sample unequal variance *t*-test and *Z*-statistics [129] to find significantly different FC for proteins and phosphosites between the different patient groups. Tyrosine phosphoproteomic data were tested for significance using linear models for microarray data (LIMMA) using the VSClust app [130]. Data from Western blotting bands were expressed as the median ± 95% confidence interval. Statistical analysis was performed using the Mann-Whitney test in Prism8.

Ethics statement

Primary AML cells were collected from AML patients after written informed consent in accordance with the Declaration of Helsinki. The storage of cells in our biobanks (REK 1759/2015) and the use of cells in the present project (REK 305/2017) were approved by the Regional Ethics Committee.

Data availability

The LC-MS/MS raw files and MaxQuant output files have been deposited to the ProteomeXchange consortium via the PRIDE partner repository [131, 132] with dataset identifier PXD019785.

AUTHOR CONTRIBUTIONS

Conceptualization, ØB; investigation and data analysis, MHV and EA; resources, FS and FB; writing original draft, MHV and ØB; review and editing of manuscript, MHV, FS, FB and ØB; funding acquisition, ØB; supervision, FS, FB and ØB.

ACKNOWLEDGMENTS

We thank Hilde Kristin Garberg, Olav Mjaavatten, Marie Hagen, Kristin Rye Paulsen and Nina Lied Larsen for excellent technical assistance.

CONFLICTS OF INTEREST

The authors declare no conflicts of interest.

FUNDING

This work was supported by Kreftforeningen, the Norwegian Cancer Society (grant no. 100933).

REFERENCES

1. Döhner H, Estey E, Grimwade D, Amadori S, Appelbaum FR, Büchner T, Dombret H, Ebert BL, Fenaux P, Larson RA, Levine RL, Lo-Coco F, Naoe T, et al. Diagnosis and management of AML in adults: 2017 ELN recommendations from an international expert panel. Blood. 2017; 129:424–47. https://doi.org/10.1182/blood-2016-08-733196 PMID:27895058

2. Nagel G, Weber D, Fromm E, Erhardt S, Lübbert M, Fiedler W, Kindler T, Krauter J, Brossart P, Kündgen A, Salih HR, Westermann J, Wulf G, et al, and German-Austrian AML Study Group (AMLSG). Epidemiological, genetic, and clinical characterization by age of newly diagnosed acute myeloid leukemia based on an

academic population-based registry study (AMLSG BiO). Ann Hematol. 2017; 96:1993–2003. https://doi.org/10.1007/s00277-017-3150-3 PMID:29090343

3. Jimenez JJ, Chale RS, Abad AC, Schally AV. Acute promyelocytic leukemia (APL): a review of the literature. Oncotarget. 2020; 11:992–1003. https://doi.org/10.18632/oncotarget.27513 PMID:32215187

4. Shallis RM, Boddu PC, Bewersdorf JP, Zeidan AM. The golden age for patients in their golden years: the progressive upheaval of age and the treatment of newly-diagnosed acute myeloid leukemia. Blood Rev. 2020; 40:100639. https://doi.org/10.1016/j.blre.2019.100639 PMID:31761380

5. Hulegårdh E, Nilsson C, Lazarevic V, Garelius H, Antunovic P, Rangert Derolf Å, Möllgård L, Uggla B, Wennström L, Wahlin A, Höglund M, Juliusson G, Stockelberg D, Lehmann S. Characterization and prognostic features of secondary acute myeloid leukemia in a population-based setting: a report from the Swedish acute leukemia registry. Am J Hematol. 2015; 90:208–14. https://doi.org/10.1002/ajh.23908 PMID:25421221

6. Papaemmanuil E, Gerstung M, Bullinger L, Gaidzik VI, Paschka P, Roberts ND, Potter NE, Heuser M, Thol F, Bolli N, Gundem G, Van Loo P, Martincorena I, et al. Genomic classification and prognosis in acute myeloid leukemia. N Engl J Med. 2016; 374:2209–21. https://doi.org/10.1056/NEJMoa1516192 PMID:27276561

7. Zjablovskaja P, Florian MC. Acute myeloid leukemia: aging and epigenetics. Cancers (Basel). 2019; 12:1S03. https://doi.org/10.3390/cancers12010103 PMID:31906064

8. Guidi N, Sacma M, Ständker L, Soller K, Marka G, Eiwen K, Weiss JM, Kirchhoff F, Weil T, Cancelas JA, Florian MC, Geiger H. Osteopontin attenuates aging-associated phenotypes of hematopoietic stem cells. EMBO J. 2017; 36:840–53. https://doi.org/10.15252/embj.201694969 PMID:28254837

9. Ho YH, Del Toro R, Rivera-Torres J, Rak J, Korn C, García-García A, Macías D, González-Gómez C, Del Monte A, Wittner M, Waller AK, Foster HR, López-Otín C, et al. Remodeling of bone marrow hematopoietic stem cell niches promotes myeloid cell expansion during premature or physiological aging. Cell Stem Cell. 2019; 25:407–18.e6. https://doi.org/10.1016/j.stem.2019.06.007 PMID:31303548

10. Kusumbe AP, Ramasamy SK, Itkin T, Mäe MA, Langen UH, Betsholtz C, Lapidot T, Adams RH. Age-dependent modulation of vascular niches for haematopoietic stem cells. Nature. 2016; 532:380–4. https://doi.org/10.1038/nature17638 PMID:27074508

11. Maryanovich M, Zahalka AH, Pierce H, Pinho S, Nakahara F, Asada N, Wei Q, Wang X, Ciero P, Xu J, Leftin A, Frenette PS. Adrenergic nerve degeneration in bone marrow drives aging of the hematopoietic stem cell niche. Nat Med. 2018; 24:782–791. https://doi.org/10.1038/s41591-018-0030-x PMID:29736022

12. Saçma M, Pospiech J, Bogeska R, de Back W, Mallm JP, Sakk V, Soller K, Marka G, Vollmer A, Karns R, Cabezas-Wallscheid N, Trumpp A, Méndez-Ferrer S, et al. Haematopoietic stem cells in perisinusoidal niches are protected from ageing. Nat Cell Biol. 2019; 21:1309–20. https://doi.org/10.1038/s41556-019-0418-y PMID:31685996

13. Florian MC, Dörr K, Niebel A, Daria D, Schrezenmeier H, Rojewski M, Filippi MD, Hasenberg A, Gunzer M, Scharffetter-Kochanek K, Zheng Y, Geiger H. Cdc42 activity regulates hematopoietic stem cell aging and rejuvenation. Cell Stem Cell. 2012; 10:520–30. https://doi.org/10.1016/j.stem.2012.04.007 PMID:22560076

14. Mejia-Ramirez E, Florian MC. Understanding intrinsic hematopoietic stem cell aging. Haematologica. 2020; 105:22–37. https://doi.org/10.3324/haematol.2018.211342 PMID:31806687

15. Ho TT, Warr MR, Adelman ER, Lansinger OM, Flach J, Verovskaya EV, Figueroa ME, Passegué E. Autophagy maintains the metabolism and function of young and old stem cells. Nature. 2017; 543:205–10. https://doi.org/10.1038/nature21388 PMID:28241143

16. Kaushik S, Cuervo AM. The coming of age of chaperone-mediated autophagy. Nat Rev Mol Cell Biol. 2018; 19:365–81. https://doi.org/10.1038/s41580-018-0001-6 PMID:29626215

17. Moran-Crusio K, Reavie LB, Aifantis I. Regulation of hematopoietic stem cell fate by the ubiquitin proteasome system. Trends Immunol. 2012; 33:357–63. https://doi.org/10.1016/j.it.2012.01.009 PMID:22349458

18. Vilchez D, Simic MS, Dillin A. Proteostasis and aging of stem cells. Trends Cell Biol. 2014; 24:161–70. https://doi.org/10.1016/j.tcb.2013.09.002 PMID:24094931

19. Florian MC, Klose M, Sacma M, Jablanovic J, Knudson L, Nattamai KJ, Marka G, Vollmer A, Soller K, Sakk V, Cabezas-Wallscheid N, Zheng Y, Mulaw MA, et al. Aging alters the epigenetic asymmetry of HSC division. PLoS Biol. 2018; 16:e2003389. https://doi.org/10.1371/journal.pbio.2003389 PMID:30235201

20. Grigoryan A, Guidi N, Senger K, Liehr T, Soller K, Marka G, Vollmer A, Markaki Y, Leonhardt H, Buske C, Lipka DB, Plass C, Zheng Y, et al. LaminA/C regulates epigenetic and chromatin architecture changes upon aging of hematopoietic stem cells. Genome Biol. 2018; 19:189. https://doi.org/10.1186/s13059-018-1557-3 PMID:30404662

21. Rao AV, Valk PJ, Metzeler KH, Acharya CR, Tuchman SA, Stevenson MM, Rizzieri DA, Delwel R, Buske C, Bohlander SK, Potti A, Löwenberg B. Age-specific differences in oncogenic pathway dysregulation and anthracycline sensitivity in patients with acute myeloid leukemia. J Clin Oncol. 2009; 27:5580–86. https://doi.org/10.1200/JCO.2009.22.2547 PMID:19858393

22. Geiger H, Zheng Y. Cdc42 and aging of hematopoietic stem cells. Curr Opin Hematol. 2013; 20:295–300. https://doi.org/10.1097/MOH.0b013e3283615aba PMID:23615056

23. Lee J, Yoon SR, Choi I, Jung H. Causes and mechanisms of hematopoietic stem cell aging. Int J Mol Sci. 2019; 20:1272. https://doi.org/10.3390/ijms20061272 PMID:30871268

24. Ren R, Ocampo A, Liu GH, Izpisua Belmonte JC. Regulation of stem cell aging by metabolism and epigenetics. Cell Metab. 2017; 26:460–74. https://doi.org/10.1016/j.cmet.2017.07.019 PMID:28826795

25. Shyh-Chang N, Daley GQ, Cantley LC. Stem cell metabolism in tissue development and aging. Development. 2013; 140:2535–47. https://doi.org/10.1242/dev.091777 PMID:23715547

26. Wiley CD, Campisi J. From ancient pathways to aging cells-connecting metabolism and cellular senescence. Cell Metab. 2016; 23:1013–21. https://doi.org/10.1016/j.cmet.2016.05.010 PMID:27304503

27. Bratic A, Larsson NG. The role of mitochondria in aging. J Clin Invest. 2013; 123:951–57. https://doi.org/10.1172/JCI64125 PMID:23454757

28. Jang JY, Blum A, Liu J, Finkel T. The role of mitochondria in aging. J Clin Invest. 2018; 128:3662–70. https://doi.org/10.1172/JCI120842 PMID:30059016

29. Min-Wen JC, Jun-Hao ET, Shyh-Chang N. Stem cell mitochondria during aging. Semin Cell Dev Biol. 2016; 52:110–18. https://doi.org/10.1016/j.semcdb.2016.02.005 PMID:26851627

30. Zhang H, Menzies KJ, Auwerx J. The role of mitochondria in stem cell fate and aging. Development. 2018; 145:dev143420. https://doi.org/10.1242/dev.143420 PMID:29654217

31. López-Otín C, Blasco MA, Partridge L, Serrano M, Kroemer G. The hallmarks of aging. Cell. 2013; 153:1194–217. https://doi.org/10.1016/j.cell.2013.05.039 PMID:23746838

32. Loeffler D, Wehling A, Schneiter F, Zhang Y, Müller-Bötticher N, Hoppe PS, Hilsenbeck O, Kokkaliaris KD, Endele M, Schroeder T. Asymmetric lysosome inheritance predicts activation of haematopoietic stem cells. Nature. 2019; 573:426–29. https://doi.org/10.1038/s41586-019-1531-6 PMID:31485073

33. Rai AK, Chen JX, Selbach M, Pelkmans L. Kinase-controlled phase transition of membraneless organelles in mitosis. Nature. 2018; 559:211–16. https://doi.org/10.1038/s41586-018-0279-8 PMID:29973724

34. Crooks GE, Hon G, Chandonia JM, Brenner SE. WebLogo: a sequence logo generator. Genome Res. 2004; 14:1188–90. https://doi.org/10.1101/gr.849004 PMID:15173120

35. Wiredja DD, Koyutürk M, Chance MR. The KSEA app: a web-based tool for kinase activity inference from quantitative phosphoproteomics. Bioinformatics. 2017; 33:3489–91. https://doi.org/10.1093/bioinformatics/btx415 PMID:28655153

36. Casado P, Rodriguez-Prados JC, Cosulich SC, Guichard S, Vanhaesebroeck B, Joel S, Cutillas PR. Kinase-substrate enrichment analysis provides insights into the heterogeneity of signaling pathway activation in leukemia cells. Sci Signal. 2013; 6:rs6. https://doi.org/10.1126/scisignal.2003573 PMID:23532336

37. Uhlén M, Fagerberg L, Hallström BM, Lindskog C, Oksvold P, Mardinoglu A, Sivertsson Å, Kampf C, Sjöstedt E, Asplund A, Olsson I, Edlund K, Lundberg E, et al. Proteomics. Tissue-based map of the human proteome. Science. 2015; 347:1260419. https://doi.org/10.1126/science.1260419 PMID:25613900

38. Licata L, Lo Surdo P, Iannuccelli M, Palma A, Micarelli E, Perfetto L, Peluso D, Calderone A, Castagnoli L, Cesareni G. SIGNOR 2.0, the SIGnaling network open resource 2.0: 2019 update. Nucleic Acids Res. 2020; 48:D504–10. https://doi.org/10.1093/nar/gkz949 PMID:31665520

39. Colaert N, Helsens K, Martens L, Vandekerckhove J, Gevaert K. Improved visualization of protein consensus sequences by iceLogo. Nat Methods. 2009; 6:786–87. https://doi.org/10.1038/nmeth1109-786 PMID:19876014

40. Sturany S, Van Lint J, Gilchrist A, Vandenheede JR, Adler G, Seufferlein T. Mechanism of activation of protein kinase D2(PKD2) by the CCK(B)/gastrin receptor. J Biol Chem. 2002; 277:29431–36. https://doi.org/10.1074/jbc.M200934200 PMID:12058027

41. LaGory EL, Sitailo LA, Denning MF. The protein kinase cdelta catalytic fragment is critical for maintenance of the G2/M DNA damage checkpoint. J Biol Chem. 2010; 285:1879–87. https://doi.org/10.1074/jbc.M109.055392 PMID:19917613

42. Timofeev O, Cizmecioglu O, Settele F, Kempf T, Hoffmann I. Cdc25 phosphatases are required for timely assembly of CDK1-cyclin B at the G2/M transition. J Biol Chem. 2010; 285:16978–90. https://doi.org/10.1074/jbc.M109.096552 PMID:20360007

43. Hossain M, Qadri SM, Xu N, Su Y, Cayabyab FS, Heit B, Liu L. Endothelial LSP1 modulates extravascular neutrophil chemotaxis by regulating nonhematopoietic vascular PECAM-1 expression. J Immunol. 2015; 195:2408–16. https://doi.org/10.4049/jimmunol.1402225 PMID:26238489

44. Meyer C, Burmeister T, Gröger D, Tsaur G, Fechina L, Renneville A, Sutton R, Venn NC, Emerenciano M, Pombo-de-Oliveira MS, Barbieri Blunck C, Almeida Lopes B, Zuna J, et al. The MLL recombinome of acute leukemias in 2017. Leukemia. 2018; 32:273–84. https://doi.org/10.1038/leu.2017.213 PMID:28701730

45. Wheatley K, Burnett AK, Goldstone AH, Gray RG, Hann IM, Harrison CJ, Rees JK, Stevens RF, Walker H. A simple, robust, validated and highly predictive index for the determination of risk-directed therapy in acute myeloid leukaemia derived from the MRC AML 10 trial. United Kingdom medical research council's adult and childhood leukaemia working parties. Br J Haematol. 1999; 107:69–79. https://doi.org/10.1046/j.1365-2141.1999.01684.x PMID:10520026

46. Paul S, Rausch CR, Jabbour EJ. The face of remission induction. Br J Haematol. 2020; 188:101–15. https://doi.org/10.1111/bjh.16353 PMID:31828798

47. Appelbaum FR, Gundacker H, Head DR, Slovak ML, Willman CL, Godwin JE, Anderson JE, Petersdorf SH. Age and acute myeloid leukemia. Blood. 2006; 107:3481–85. https://doi.org/10.1182/blood-2005-09-3724 PMID:16455952

48. Lancet JE, Cortes JE, Hogge DE, Tallman MS, Kovacsovics TJ, Damon LE, Komrokji R, Solomon SR, Kolitz JE, Cooper M, Yeager AM, Louie AC, Feldman EJ. Phase 2 trial of CPX-351, a fixed 5:1 molar ratio of cytarabine/daunorubicin, vs cytarabine/daunorubicin in older adults with untreated AML. Blood. 2014; 123:3239–46. https://doi.org/10.1182/blood-2013-12-540971 PMID:24687088

49. Webster JA, Pratz KW. Acute myeloid leukemia in the elderly: therapeutic options and choice. Leuk Lymphoma. 2018; 59:274–87. https://doi.org/10.1080/10428194.2017.1330956 PMID:28573892

50. Burnett AK, Russell NH, Hills RK, Kell J, Cavenagh J, Kjeldsen L, McMullin MF, Cahalin P, Dennis M, Friis L, Thomas IF, Milligan D, Clark RE, and UK NCRI AML Study Group. A randomized comparison of daunorubicin 90 mg/m2 vs 60 mg/m2 in AML induction: results from the UK NCRI AML17 trial in 1206 patients. Blood. 2015; 125:3878–85. https://doi.org/10.1182/blood-2015-01-623447 PMID:25833957

51. Löwenberg B, Ossenkoppele GJ, van Putten W, Schouten HC, Graux C, Ferrant A, Sonneveld P, Maertens J, Jongen-Lavrencic M, von Lilienfeld-Toal M, Biemond BJ, Vellenga E, van Marwijk Kooy M, et al, Dutch-Belgian Cooperative Trial Group for Hemato-Oncology (HOVON), German AML Study Group (AMLSG), and Swiss Group for Clinical Cancer Research (SAKK) Collaborative Group. High-dose daunorubicin in older patients with acute myeloid leukemia. N Engl J Med. 2009; 361:1235–48. https://doi.org/10.1056/NEJMoa0901409 PMID:19776405

52. Keiffer G, Palmisiano N. Acute myeloid leukemia: update on upfront therapy in elderly patients. Curr Oncol Rep. 2019; 21:71. https://doi.org/10.1007/s11912-019-0823-1 PMID:31250135

53. Bruserud O, Gjertsen BT, Foss B, Huang TS. New strategies in the treatment of acute myelogenous leukemia (AML): in vitro culture of aml cells—the present use in experimental studies and the possible

importance for future therapeutic approaches. Stem Cells. 2001; 19:1–11.
https://doi.org/10.1634/stemcells.19-1-1
PMID:11209086

54. Gjertsen BT, Øyan AM, Marzolf B, Hovland R, Gausdal G, Døskeland SO, Dimitrov K, Golden A, Kalland KH, Hood L, Bruserud Ø. Analysis of acute myelogenous leukemia: preparation of samples for genomic and proteomic analyses. J Hematother Stem Cell Res. 2002; 11:469–81.
https://doi.org/10.1089/15258160260090933
PMID:12183832

55. de Jonge HJ, Valk PJ, de Bont ES, Schuringa JJ, Ossenkoppele G, Vellenga E, Huls G. Prognostic impact of white blood cell count in intermediate risk acute myeloid leukemia: relevance of mutated NPM1 and FLT3-ITD. Haematologica. 2011; 96:1310–17.
https://doi.org/10.3324/haematol.2011.040592
PMID:21606167

56. Feng S, Zhou L, Zhang X, Tang B, Zhu X, Liu H, Sun Z, Zheng C. Impact Of ELN Risk Stratification, Induction Chemotherapy Regimens And Hematopoietic Stem Cell Transplantation On Outcomes In Hyperleukocytic Acute Myeloid Leukemia With Initial White Blood Cell Count More Than 100 × 109/L. Cancer Manag Res. 2019; 11:9495–9503.
https://doi.org/10.2147/CMAR.S225123
PMID:31807075

57. How J, Sykes J, Gupta V, Yee KW, Schimmer AD, Schuh AC, Minden MD, Kamel-Reid S, Brandwein JM. Influence of FLT3-internal tandem duplication allele burden and white blood cell count on the outcome in patients with intermediate-risk karyotype acute myeloid leukemia. Cancer. 2012; 118:6110–17.
https://doi.org/10.1002/cncr.27683 PMID:22736495

58. Arber DA, Orazi A, Hasserjian R, Thiele J, Borowitz MJ, Le Beau MM, Bloomfield CD, Cazzola M, Vardiman JW. The 2016 revision to the world health organization classification of myeloid neoplasms and acute leukemia. Blood. 2016; 127:2391–405.
https://doi.org/10.1182/blood-2016-03-643544
PMID:27069254

59. Reuss-Borst MA, Klein G, Waller HD, Müller CA. Differential expression of adhesion molecules in acute leukemia. Leukemia. 1995; 9:869–74.
PMID:7539515

60. Brenner AK, Aasebø E, Hernandez-Valladares M, Selheim F, Berven F, Grønningsæter IS, Bartaula-Brevik S, Bruserud Ø. The capacity of long-term in vitro proliferation of acute myeloid leukemia cells supported only by exogenous cytokines is associated with a patient subset with adverse outcome. Cancers (Basel). 2019; 11:73.
https://doi.org/10.3390/cancers11010073
PMID:30634713

61. Nepstad I, Hatfield KJ, Tvedt TH, Reikvam H, Bruserud Ø. Clonal heterogeneity reflected by PI3K-AKT-mTOR signaling in human acute myeloid leukemia cells and its association with adverse prognosis. Cancers (Basel). 2018; 10:332.
https://doi.org/10.3390/cancers10090332
PMID:30223538

62. Nilsson C, Hulegårdh E, Garelius H, Möllgård L, Brune M, Wahlin A, Lenhoff S, Frödin U, Remberger M, Höglund M, Juliusson G, Stockelberg D, Lehmann S. Secondary acute myeloid leukemia and the role of allogeneic stem cell transplantation in a population-based setting. Biol Blood Marrow Transplant. 2019; 25:1770–78.
https://doi.org/10.1016/j.bbmt.2019.05.038
PMID:31176789

63. Reikvam H, Aasebø E, Brenner AK, Bartaula-Brevik S, Grønningsæter IS, Forthun RB, Hovland R, Bruserud Ø. High constitutive cytokine release by primary human acute myeloid leukemia cells is associated with a specific intercellular communication phenotype. J Clin Med. 2019; 8:970.
https://doi.org/10.3390/jcm8070970 PMID:31277464

64. Tsykunova G, Reikvam H, Hovland R, Bruserud Ø. The surface molecule signature of primary human acute myeloid leukemia (AML) cells is highly associated with NPM1 mutation status. Leukemia. 2012; 26:557–59.
https://doi.org/10.1038/leu.2011.243 PMID:21904378

65. Aasebø E, Berven FS, Bartaula-Brevik S, Stokowy T, Hovland R, Vaudel M, Døskeland SO, McCormack E, Batth TS, Olsen JV, Bruserud Ø, Selheim F, Hernandez-Valladares M. Proteome and Phosphoproteome Changes Associated with Prognosis in Acute Myeloid Leukemia. Cancers (Basel). 2020; 12:709.
https://doi.org/10.3390/cancers12030709
PMID:32192169

66. Aasebø E, Berven FS, Hovland R, Døskeland SO, Bruserud Ø, Selheim F, Hernandez-Valladares M. The Progression of Acute Myeloid Leukemia from First Diagnosis to Chemoresistant Relapse: A Comparison of Proteomic and Phosphoproteomic Profiles. Cancers (Basel). 2020; 12:1466.
https://doi.org/10.3390/cancers12061466
PMID:32512867

67. Yang CK, Wang XK, Liao XW, Han CY, Yu TD, Qin W, Zhu GZ, Su H, Yu L, Liu XG, Lu SC, Chen ZW, Liu Z, et al. Aldehyde dehydrogenase 1 (ALDH1) isoform expression and potential clinical implications in hepatocellular carcinoma. PLoS One. 2017; 12:e0182208.
https://doi.org/10.1371/journal.pone.0182208
PMID:28792511

68. Li R, Zhao Z, Sun M, Luo J, Xiao Y. ALDH2 gene polymorphism in different types of cancers and its clinical significance. Life Sci. 2016; 147:59–66. https://doi.org/10.1016/j.lfs.2016.01.028 PMID:26804999

69. Hira A, Yabe H, Yoshida K, Okuno Y, Shiraishi Y, Chiba K, Tanaka H, Miyano S, Nakamura J, Kojima S, Ogawa S, Matsuo K, Takata M, Yabe M. Variant ALDH2 is associated with accelerated progression of bone marrow failure in Japanese fanconi anemia patients. Blood. 2013; 122:3206–09. https://doi.org/10.1182/blood-2013-06-507962 PMID:24037726

70. Hou H, Li D, Gao J, Gao L, Lu Q, Hu Y, Wu S, Chu X, Yao Y, Wan L, Ling J, Pan J, Xu G, Hu S. Proteomic profiling and bioinformatics analysis identify key regulators during the process from fanconi anemia to acute myeloid leukemia. Am J Transl Res. 2020; 12:1415–27. PMID:32355551

71. Langevin F, Crossan GP, Rosado IV, Arends MJ, Patel KJ. Fancd2 counteracts the toxic effects of naturally produced aldehydes in mice. Nature. 2011; 475:53–58. https://doi.org/10.1038/nature10192 PMID:21734703

72. Yabe M, Koike T, Ohtsubo K, Imai E, Morimoto T, Takakura H, Koh K, Yoshida K, Ogawa S, Ito E, Okuno Y, Muramatsu H, Kojima S, et al. Associations of complementation group, ALDH2 genotype, and clonal abnormalities with hematological outcome in Japanese patients with fanconi anemia. Ann Hematol. 2019; 98:271–80. https://doi.org/10.1007/s00277-018-3517-0 PMID:30368588

73. Venton G, Pérez-Alea M, Baier C, Fournet G, Quash G, Labiad Y, Martin G, Sanderson F, Poullin P, Suchon P, Farnault L, Nguyen C, Brunet C, et al. Aldehyde dehydrogenases inhibition eradicates leukemia stem cells while sparing normal progenitors. Blood Cancer J. 2016; 6:e469. https://doi.org/10.1038/bcj.2016.78 PMID:27611922

74. Yusuf RZ, Saez B, Sharda A, van Gastel N, Yu VW, Baryawno N, Scadden EW, Acharya S, Chattophadhyay S, Huang C, Viswanathan V, S'aulis D, Cobert J, et al. Aldehyde dehydrogenase 3a2 protects AML cells from oxidative death and the synthetic lethality of ferroptosis inducers. Blood. 2020; 136:1303–16. https://doi.org/10.1182/blood.2019001808 PMID:32458004

75. Bista R, Lee DW, Pepper OB, Azorsa DO, Arceci RJ, Aleem E. Disulfiram overcomes bortezomib and cytarabine resistance in down-syndrome-associated acute myeloid leukemia cells. J Exp Clin Cancer Res. 2017; 36:22. https://doi.org/10.1186/s13046-017-0493-5 PMID:28143565

76. Moreb JS, Ucar D, Han S, Amory JK, Goldstein AS, Ostmark B, Chang LJ. The enzymatic activity of human aldehyde dehydrogenases 1A2 and 2 (ALDH1A2 and ALDH2) is detected by aldefluor, inhibited by diethylaminobenzaldehyde and has significant effects on cell proliferation and drug resistance. Chem Biol Interact. 2012; 195:52–60. https://doi.org/10.1016/j.cbi.2011.10.007 PMID:22079344

77. Ran D, Schubert M, Pietsch L, Taubert I, Wuchter P, Eckstein V, Bruckner T, Zoeller M, Ho AD. Aldehyde dehydrogenase activity among primary leukemia cells is associated with stem cell features and correlates with adverse clinical outcomes. Exp Hematol. 2009; 37:1423–34. https://doi.org/10.1016/j.exphem.2009.10.001 PMID:19819294

78. Yang W, Xie J, Hou R, Chen X, Xu Z, Tan Y, Ren F, Zhang Y, Xu J, Chang J, Wang H. Disulfiram/cytarabine eradicates a subset of acute myeloid leukemia stem cells with high aldehyde dehydrogenase expression. Leuk Res. 2020; 92:106351. https://doi.org/10.1016/j.leukres.2020.106351 PMID:32224355

79. Yang L, Chen WM, Dao FT, Zhang YH, Wang YZ, Chang Y, Liu YR, Jiang Q, Zhang XH, Liu KY, Huang XJ, Qin YZ. High aldehyde dehydrogenase activity at diagnosis predicts relapse in patients with t(8;21) acute myeloid leukemia. Cancer Med. 2019; 8:5459–67. https://doi.org/10.1002/cam4.2422 PMID:31364309

80. Torrebadell M, Díaz-Beyá M, Kalko SG, Pratcorona M, Nomdedeu J, Navarro A, Gel B, Brunet S, Sierra J, Camós M, Esteve J. A 4-gene expression prognostic signature might guide post-remission therapy in patients with intermediate-risk cytogenetic acute myeloid leukemia. Leuk Lymphoma. 2018; 59:2394–404. https://doi.org/10.1080/10428194.2017.1422859 PMID:29390924

81. Yang X, Yao R, Wang H. Update of ALDH as a potential biomarker and therapeutic target for AML. Biomed Res Int. 2018; 2018:9192104. https://doi.org/10.1155/2018/9192104 PMID:29516013

82. Goodson HV, Jonasson EM. Microtubules and microtubule-associated proteins. Cold Spring Harb Perspect Biol. 2018; 10:a022608. https://doi.org/10.1101/cshperspect.a022608 PMID:29858272

83. Hohmann T, Dehghani F. The cytoskeleton-a complex

interacting meshwork. Cells. 2019; 8:362. https://doi.org/10.3390/cells8040362 PMID:31003495

84. Duellberg C, Cade NI, Surrey T. Microtubule aging probed by microfluidics-assisted tubulin washout. Mol Biol Cell. 2016; 27:3563–73. https://doi.org/10.1091/mbc.E16-07-0548 PMID:27489342

85. Lai WF, Wong WT. Roles of the actin cytoskeleton in aging and age-associated diseases. Ageing Res Rev. 2020; 58:101021. https://doi.org/10.1016/j.arr.2020.101021 PMID:31968269

86. Xu P, Crawford M, Way M, Godovac-Zimmermann J, Segal AW, Radulovic M. Subproteome analysis of the neutrophil cytoskeleton. Proteomics. 2009; 9:2037–49. https://doi.org/10.1002/pmic.200800674 PMID:19294702

87. Löwenberg B, van Putten WL, Touw IP, Delwel R, Santini V. Autonomous proliferation of leukemic cells in vitro as a determinant of prognosis in adult acute myeloid leukemia. N Engl J Med. 1993; 328:614–19. https://doi.org/10.1056/NEJM199303043280904 PMID:8429853

88. Hunter AE, Rogers SY, Roberts IA, Barrett AJ, Russell N. Autonomous growth of blast cells is associated with reduced survival in acute myeloblastic leukemia. Blood. 1993; 82:899–903. PMID:8338952

89. Rombouts WJ, Löwenberg B, van Putten WL, Ploemacher RE. Improved prognostic significance of cytokine-induced proliferation in vitro in patients with de novo acute myeloid leukemia of intermediate risk: impact of internal tandem duplications in the Flt3 gene. Leukemia. 2001; 15:1046–53. https://doi.org/10.1038/sj.leu.2402157 PMID:11455972

90. Yan Y, Wieman EA, Guan X, Jakubowski AA, Steinherz PG, O'Reilly RJ. Autonomous growth potential of leukemia blast cells is associated with poor prognosis in human acute leukemias. J Hematol Oncol. 2009; 2:51. https://doi.org/10.1186/1756-8722-2-51 PMID:20040095

91. Choudary I, Barr PM, Friedberg J. Recent advances in the development of aurora kinases inhibitors in hematological Malignancies. Ther Adv Hematol. 2015; 6:282–94. https://doi.org/10.1177/2040620715607415 PMID:26622997

92. Tsykunova G, Reikvam H, Ahmed AB, Nepstad I, Gjertsen BT, Bruserud Ø. Targeting of polo-like kinases and their cross talk with aurora kinases—possible therapeutic strategies in human acute myeloid leukemia? Expert Opin Investig Drugs. 2012; 21:587–603. https://doi.org/10.1517/13543784.2012.668525 PMID:22424119

93. Bechtold M, Schultz J, Bogdan S. FHOD proteins in actin dynamics—a formin' class of its own. Small GTPases. 2014; 5:11. https://doi.org/10.4161/21541248.2014.973765 PMID:25483300

94. Eisenmann KM, Dykema KJ, Matheson SF, Kent NF, DeWard AD, West RA, Tibes R, Furge KA, Alberts AS. 5q- myelodysplastic syndromes: chromosome 5q genes direct a tumor-suppression network sensing actin dynamics. Oncogene. 2009; 28:3429–41. https://doi.org/10.1038/onc.2009.207 PMID:19597464

95. Zhang Y, Hu C. Anticancer activity of bisindole alkaloids derived from natural sources and synthetic bisindole hybrids. Arch Pharm (Weinheim). 2020; 353:e2000092. https://doi.org/10.1002/ardp.202000092 PMID:32468606

96. Thoms JA, Beck D, Pimanda JE. Transcriptional networks in acute myeloid leukemia. Genes Chromosomes Cancer. 2019; 58:859–74. https://doi.org/10.1002/gcc.22794 PMID:31369171

97. Assi SA, Imperato MR, Coleman DJ, Pickin A, Potluri S, Ptasinska A, Chin PS, Blair H, Cauchy P, James SR, Zacarias-Cabeza J, Gilding LN, Beggs A, et al. Subtype-specific regulatory network rewiring in acute myeloid leukemia. Nat Genet. 2019; 51:151–62. https://doi.org/10.1038/s41588-018-0270-1 PMID:30420649

98. Marais A, Ji Z, Child ES, Krause E, Mann DJ, Sharrocks AD. Cell cycle-dependent regulation of the forkhead transcription factor FOXK2 by CDK·cyclin complexes. J Biol Chem. 2010; 285:35728–39. https://doi.org/10.1074/jbc.M110.154005 PMID:20810654

99. McNair C, Xu K, Mandigo AC, Benelli M, Leiby B, Rodrigues D, Lindberg J, Gronberg H, Crespo M, De Laere B, Dirix L, Visakorpi T, Li F, et al. Differential impact of RB status on E2F1 reprogramming in human cancer. J Clin Invest. 2018; 128:341–58. https://doi.org/10.1172/JCI93566 PMID:29202480

100. Strom DK, Cleveland JL, Chellappan S, Nip J, Hiebert SW. E2F-1 and E2F-3 are functionally distinct in their ability to promote myeloid cell cycle progression and block granulocyte differentiation. Cell Growth Differ. 1998; 9:59–69. PMID:9438389

101. Ou HL, Schumacher B. DNA damage responses and p53 in the aging process. Blood. 2018; 131:488–95. https://doi.org/10.1182/blood-2017-07-746396 PMID:29141944

102. Rufini A, Tucci P, Celardo I, Melino G. Senescence and aging: the critical roles of p53. Oncogene. 2013; 32:5129–43. https://doi.org/10.1038/onc.2012.640 PMID:23416979

103. Wu D, Prives C. Relevance of the p53-MDM2 axis to aging. Cell Death Differ. 2018; 25:169–79. https://doi.org/10.1038/cdd.2017.187 PMID:29192902

104. Bendre S, Rondelet A, Hall C, Schmidt N, Lin YC, Brouhard GJ, Bird AW. GTSE1 tunes microtubule stability for chromosome alignment and segregation by inhibiting the microtubule depolymerase MCAK. J Cell Biol. 2016; 215:631–47. https://doi.org/10.1083/jcb.201606081 PMID:27881713

105. Chu X, Chen X, Wan Q, Zheng Z, Du Q. Nuclear mitotic apparatus (NuMA) interacts with and regulates astrin at the mitotic spindle. J Biol Chem. 2016; 291:20055–67. https://doi.org/10.1074/jbc.M116.724831 PMID:27462074

106. Schwind S, Jentzsch M, Bach E, Stasik S, Thiede C, Platzbecker U. Use of minimal residual disease in acute myeloid leukemia therapy. Curr Treat Options Oncol. 2020; 21:8. https://doi.org/10.1007/s11864-019-0695-5 PMID:32002673

107. Venditti A, Peter Gale R, Buccisano F, Ossenkoppele G. Should persons with acute myeloid leukemia (AML) in 1st histological complete remission who are measurable residual disease (MRD) test positive receive an allotransplant? Leukemia. 2020; 34:963–65. https://doi.org/10.1038/s41375-020-0780-6 PMID:32132654

108. Löwenberg B, Pabst T, Maertens J, van Norden Y, Biemond BJ, Schouten HC, Spertini O, Vellenga E, Graux C, Havelange V, de Greef GE, de Weerdt O, Legdeur MJ, et al, and Dutch-Belgian Hemato-Oncology Cooperative Group (HOVON) and Swiss Group for Clinical Cancer Research (SAKK). Therapeutic value of clofarabine in younger and middle-aged (18-65 years) adults with newly diagnosed AML. Blood. 2017; 129:1636–45. https://doi.org/10.1182/blood-2016-10-740613 PMID:28049642

109. Ossenkoppele GJ, Breems DA, Stuessi G, van Norden Y, Bargetzi M, Biemond BJ, A von dem Borne P, Chalandon Y, Cloos J, Deeren D, Fehr M, Gjertsen B, Graux C, et al. Lenalidomide added to standard intensive treatment for older patients with AML and high-risk MDS. Leukemia. 2020; 34:1751–1759. https://doi.org/10.1038/s41375-020-0725-0 PMID:32020044

110. Hernandez-Valladares M, Aasebø E, Mjaavatten O, Vaudel M, Bruserud Ø, Berven F, Selheim F. Reliable FASP-based procedures for optimal quantitative proteomic and phosphoproteomic analysis on samples from acute myeloid leukemia patients. Biol Proced Online. 2016; 18:13. https://doi.org/10.1186/s12575-016-0043-0 PMID:27330413

111. Aasebø E, Vaudel M, Mjaavatten O, Gausdal G, Van der Burgh A, Gjertsen BT, Døskeland SO, Bruserud O, Berven FS, Selheim F. Performance of super-SILAC based quantitative proteomics for comparison of different acute myeloid leukemia (AML) cell lines. Proteomics. 2014; 14:1971–76. https://doi.org/10.1002/pmic.201300448 PMID:25044641

112. Wiśniewski JR, Zougman A, Nagaraj N, Mann M. Universal sample preparation method for proteome analysis. Nat Methods. 2009; 6:359–62. https://doi.org/10.1038/nmeth.1322 PMID:19377485

113. Kulak NA, Pichler G, Paron I, Nagaraj N, Mann M. Minimal, encapsulated proteomic-sample processing applied to copy-number estimation in eukaryotic cells. Nat Methods. 2014; 11:319–24. https://doi.org/10.1038/nmeth.2834 PMID:24487582

114. Cox J, Mann M. MaxQuant enables high peptide identification rates, individualized p.p.b.-range mass accuracies and proteome-wide protein quantification. Nat Biotechnol. 2008; 26:1367–72. https://doi.org/10.1038/nbt.1511 PMID:19029910

115. Cox J, Matic I, Hilger M, Nagaraj N, Selbach M, Olsen JV, Mann M. A practical guide to the MaxQuant computational platform for SILAC-based quantitative proteomics. Nat Protoc. 2009; 4:698–705. https://doi.org/10.1038/nprot.2009.36 PMID:19373234

116. Cox J, Neuhauser N, Michalski A, Scheltema RA, Olsen JV, Mann M. Andromeda: a peptide search engine integrated into the MaxQuant environment. J Proteome Res. 2011; 10:1794–805. https://doi.org/10.1021/pr101065j PMID:21254760

117. Tyanova S, Temu T, Sinitcyn P, Carlson A, Hein MY, Geiger T, Mann M, Cox J. The perseus computational platform for comprehensive analysis of (prote)omics data. Nat Methods. 2016; 13:731–40. https://doi.org/10.1038/nmeth.3901 PMID:27348712

118. Schölz C, Lyon D, Refsgaard JC, Jensen LJ, Choudhary C, Weinert BT. Avoiding abundance bias in the functional annotation of post-translationally modified proteins. Nat Methods. 2015; 12:1003–04. https://doi.org/10.1038/nmeth.3621 PMID:26513550

119. Hornbeck PV, Zhang B, Murray B, Kornhauser JM, Latham V, Skrzypek E. PhosphoSitePlus, 2014: mutations, PTMs and recalibrations. Nucleic Acids Res. 2015; 43:D512–20. https://doi.org/10.1093/nar/gku1267 PMID:25514926

120. Linding R, Jensen LJ, Ostheimer GJ, van Vugt MA, Jørgensen C, Miron IM, Diella F, Colwill K, Taylor L, Elder K, Metalnikov P, Nguyen V, Pasculescu A, et al. Systematic discovery of in vivo phosphorylation networks. Cell. 2007; 129:1415–26. https://doi.org/10.1016/j.cell.2007.05.052 PMID:17570479

121. Szklarczyk D, Morris JH, Cook H, Kuhn M, Wyder S, Simonovic M, Santos A, Doncheva NT, Roth A, Bork P, Jensen LJ, von Mering C. The STRING database in 2017: quality-controlled protein-protein association networks, made broadly accessible. Nucleic Acids Res. 2017; 45:D362–68. https://doi.org/10.1093/nar/gkw937 PMID:27924014

122. Shannon P, Markiel A, Ozier O, Baliga NS, Wang JT, Ramage D, Amin N, Schwikowski B, Ideker T. Cytoscape: a software environment for integrated models of biomolecular interaction networks. Genome Res. 2003; 13:2498–504. https://doi.org/10.1101/gr.1239303 PMID:14597658

123. Nepusz T, Yu H, Paccanaro A. Detecting overlapping protein complexes in protein-protein interaction networks. Nat Methods. 2012; 9:471–72. https://doi.org/10.1038/nmeth.1938 PMID:22426491

124. Doncheva NT, Morris JH, Gorodkin J, Jensen LJ. Cytoscape StringApp: network analysis and visualization of proteomics data. J Proteome Res. 2019; 18:623–32. https://doi.org/10.1021/acs.jproteome.8b00702 PMID:30450911

125. Blucher AS, McWeeney SK, Stein L, Wu G. Visualization of drug target interactions in the contexts of pathways and networks with ReactomeFIViz. F1000Res. 2019; 8:908. https://doi.org/10.12688/f1000research.19592.1 PMID:31372215

126. Wu G, Dawson E, Duong A, Haw R, Stein L. ReactomeFIViz: a cytoscape app for pathway and network-based data analysis. F1000Res. 2014; 3:146. https://doi.org/10.12688/f1000research.4431.2 PMID:25309732

127. Hulsen T, de Vlieg J, Alkema W. BioVenn - a web application for the comparison and visualization of biological lists using area-proportional venn diagrams. BMC Genomics. 2008; 9:488. https://doi.org/10.1186/1471-2164-9-488 PMID:18925949

128. Schneider CA, Rasband WS, Eliceiri KW. NIH image to ImageJ: 25 years of image analysis. Nat Methods. 2012; 9:671–75. https://doi.org/10.1038/nmeth.2089 PMID:22930834

129. Arntzen MØ, Koehler CJ, Barsnes H, Berven FS, Treumann A, Thiede B. IsobariQ: software for isobaric quantitative proteomics using IPTL, iTRAQ, and TMT. J Proteome Res. 2011; 10:913–20. https://doi.org/10.1021/pr1009977 PMID:21067241

130. Schwämmle V, Jensen ON. VSClust: feature-based variance-sensitive clustering of omics data. Bioinformatics. 2018; 34:2965–72. https://doi.org/10.1093/bioinformatics/bty224 PMID:29635359

131. Vizcaíno JA, Deutsch EW, Wang R, Csordas A, Reisinger F, Ríos D, Dianes JA, Sun Z, Farrah T, Bandeira N, Binz PA, Xenarios I, Eisenacher M, et al. ProteomeXchange provides globally coordinated proteomics data submission and dissemination. Nat Biotechnol. 2014; 32:223–26. https://doi.org/10.1038/nbt.2839 PMID:24727771

132. Vizcaíno JA, Csordas A, del-Toro N, Dianes JA, Griss J, Lavidas I, Mayer G, Perez-Riverol Y, Reisinger F, Ternent T, Xu QW, Wang R, Hermjakob H. 2016 update of the PRIDE database and its related tools. Nucleic Acids Res. 2016; 44:D447–56. https://doi.org/10.1093/nar/gkv1145 PMID:26527722

SUPPLEMENTARY MATERIALS

Supplementary Figures

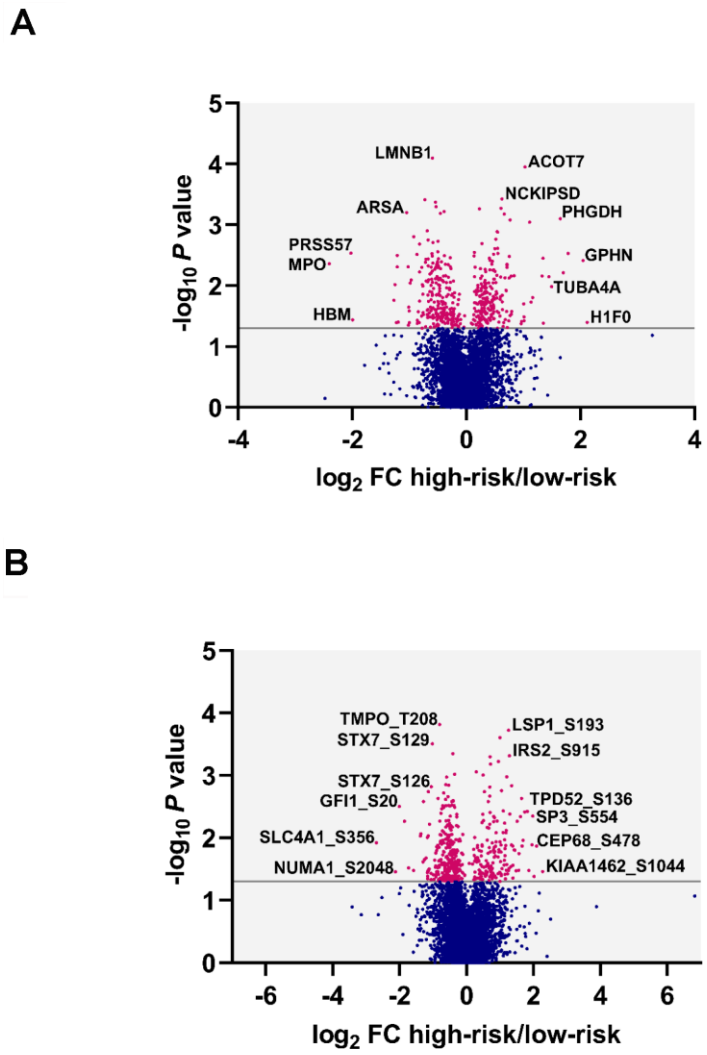

Supplementary Figure 1. Volcano plot analyses of the data from the high-risk *vs* low-risk cohort. Points (in magenta) above the non-axial horizontal grey line represent proteins or phosphosites with significantly different abundances or phosphorylation ($P < 0.05$), respectively. (**A**) All proteins with at least 5 quantitative values in each group were used in the analysis. (**B**) All phosphosites with at least 5 quantitative values in each group were used in the analysis.

A

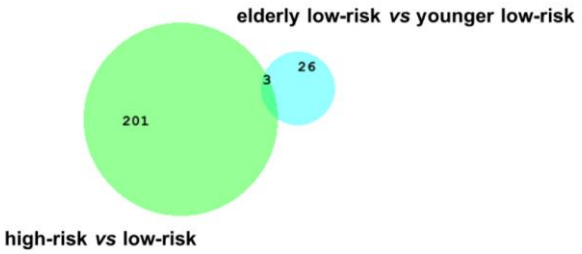

Protein	FC elderly low-risk *vs* younger low-risk	FC high-risk *vs* low-risk
ALDH2	1.9985	1.7844
UFSP2	0.4986	-0.4933
BAG2	-0.9124	1.4456

B

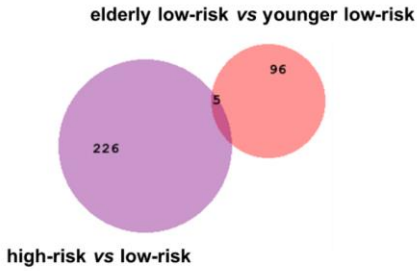

Phosphosite	FC elderly low-risk *vs* younger low-risk	FC high-risk *vs* low-risk
LSP1_S177	1.0748	0.9508
TMPO_S159	0.6759	-1.1676
CDK1_Y15	-1.0066	0.7270
CDK2_Y15	-1.0066	0.7270
ESCO2_S75	-1.7257	1.4278

Supplementary Figure 2. Venn diagrams of regulated proteins and phosphoproteins in the studies of elderly low-risk *vs* younger low-risk, and high-risk *vs* all low-risk patients. (**A**) Overlap of 29 and 204 regulated proteins in the elderly low-risk *vs* younger low-risk, and high-risk *vs* low-risk studies, respectively, with table of the fold change (FC) values of overlapped proteins obtained in both studies. (**B**) Overlap of 101 and 231 unique differentially regulated phosphorylation sites in the elderly low-risk *vs* younger low-risk, and high-risk *vs* low-risk studies, respectively, with table of the FC values of overlapped phosphosites obtained in both studies.

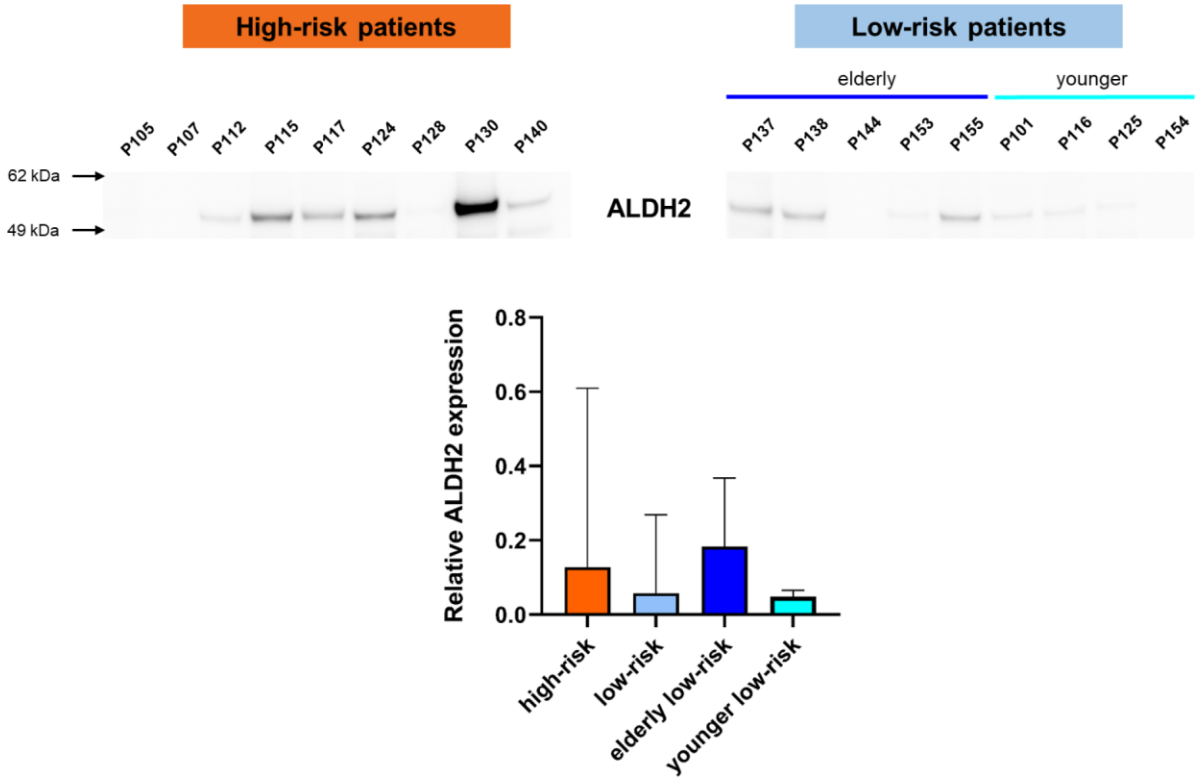

Supplementary Figure 3. Western blots of sample lysates from nine high-risk and nine low-risk patients to study the activity of ALDH2. Band intensities of ALDH2 protein were normalized before statistical analysis. Data from Western blot bands were expressed as the median ± 95% confidence interval in the bar plots. Band intensities from the high-risk and low-risk as well as from elderly low-risk and younger low-risk samples were compared using the Mann-Whitney test. None of the comparisons were statistically significant. Western blots were not replicated.

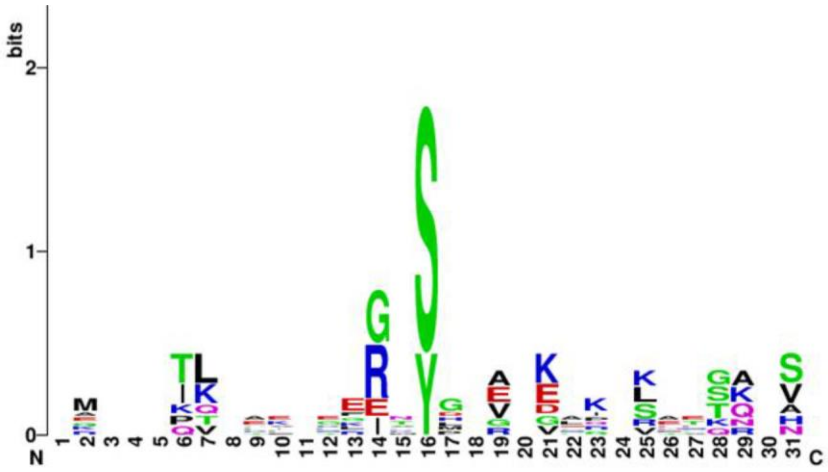

Supplementary Figure 4. Sequence logo analysis of the phosphoprotein Cluster 1 showed in Figure 5C on the main text. Thirty-one amino acid sequence windows surrounding the phosphorylation sites (located on position 16 on the x-axis) described in the protein cluster.

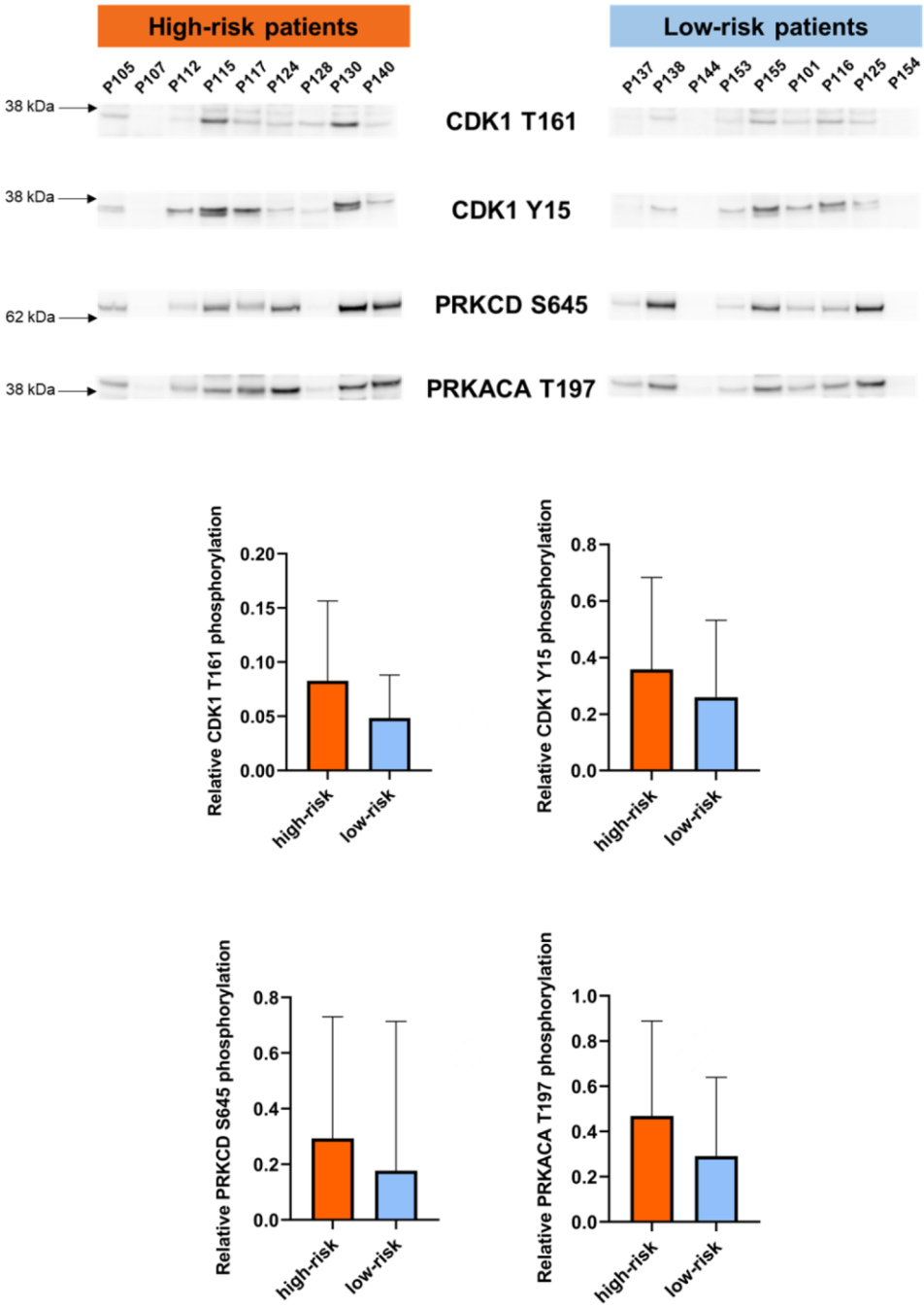

Supplementary Figure 5. Western blots of sample lysates from nine high-risk and nine low-risk patients to study the activity of CDK1, PRKCD and PRKACA. Band intensities of phosphorylated proteins were normalized before statistical analysis. Data from Western blot bands were expressed as the median ± 95% confidence interval in the bar plots. Band intensities from the high-risk and low-risk samples were compared using the Mann-Whitney test. None of the comparisons were statistically significant. Western blots were not replicated.

Supplementary Tables

Please browse Full Text version to see the data of Supplementary Tables 4–7.

Supplementary Table 1. Clinical and biological characteristics of individual patients included in the study.

ID	Sex	Age	FAB	CD34	Karyotype	*FLT3*	*NPM1*
High-risk patients, i.e. adverse cytogenetic abnormalities							
A1-P105	F	64	M1	+	Complex[2]	WT	WT
A2-P112	F	51	M0	+	Complex	WT	WT
A3-P114	M	72	M1	+	Complex	WT	-
A4-P117	F	64	M1	+	Complex	ITD	WT
A5-P122	M	84	M1	+	Complex	WT	WT
A6-P130	M	78	M0	-	Complex	WT	WT
A7-P133	M	74	M4	-	Complex	WT	-
A8-P134	M	80	M1	+	Complex	-	-
A9-P140	F	50	M2	+	Complex	WT	WT
A10-P128	M	77	M2	+	Complex	ITD	WT
A11-P115	F	87	M0	+	del 5	WT	WT
A12-P107	M	73	M2	+	Monosomal	ITD	WT
A13-P123	M	81	M2	-	-7	WT	WT
A14-P124	M	76	M5	+	del 12, -7	WT	WT
A15-P129	M	63	M5	+	-7	WT	WT
Low-risk patients, i.e. favorable genetic abnormalities							
F1-P110	F	67	M4	+	t(16;16), +22	-	-
F2-P116	M	36	M5	+	inv16, +8, +22	ITD	WT
F3-P139	M	66	M5	+	t(16;16)	WT	WT
F4-P141	M	79	M2	-	inv16, del 7	WT	WT
F5-P127	M	41	M1	+	t(8;21), del 9, -3, -20, -22	WT	WT
F6-P131	F	33	M1	+	t(8;21)	WT	WT
F7-P137	F	74	M4	+	t(8;21)	ITD	WT
F8-P144	F	66	M4	+	t(8;21)	WT	WT
F9-P154	M	47	M4	-	t(8;21)	WT	WT
F10-P101	M	50	M2	-	Normal	WT	INS
F11-P118	F	61	M5	-	Normal	WT	INS
F12-P120	F	68	M5	-	Normal	WT	INS
F13-P125	M	64	M5	-	Normal	WT	INS
F14-P138	M	65	M4	-	Normal	WT	INS
F15-P143	M	64	M1	+	Normal	WT	INS
F16-P153	F	70	M4	+	Normal	WT	INS
F17-P155[3]	F	71	M0	-	Normal	ITD^{low}	INS
F18-P142[4]	M	33	M2	+	Normal	WT	WT

The table presents individually patient characteristics (sex, gender), morphological (FAB classification) and molecular signs of differentiation (CD34 expression), karyotype and *FLT3*/*NPM1* mutational status[1].

[1]Abbreviations: FAB, French-American-British; INS, a 4 bp-insertion/duplication; ITD, internal tandem duplication; WT, wild-type; -, not determined.

[2]Defined as ≥ 3 cytogenetic abnormalities.

[3]The patient had a low ITD ratio and could therefore be classified as having a favorable prognosis. He was initially classified as ITD negative but later reclassified based on a new analysis.

[4]This patient has *CEBPA* mutation.

Supplementary Table 2. Patient treatment and survival.

ID	Treatment[1]	Survival (months)
	High risk patients, i.e. adverse cytogenetic abnormalities	
A1-P105	Best supportive care	<1
A2-P112	AML-stabilizing therapy based on ATRA and valproic acid	3
A3-P114	AML-stabilizing therapy based on ATRA and valproic acid	13
A4-P117	Best supportive care	3
A5-P122	AML-stabilizing therapy based on ATRA and valproic acid	5
A6-P130	Valproic acid plus hydroxyurea	3
A7-P133	Best supportive care	<1
A8-P134	AML-stabilizing therapy based on ATRA and valproic acid	1
A9-P140	Intensive chemotherapy followed by allogeneic SCT	>46[2]
A10-P128	Best supportive care	<1
A11-P115	ATRA, valproic acid, low-dose cytarabine	<1
A12-P107	Best supportive care	2
A13-P123	ATRA, valproic acid, low-dose cytarabine	16
A14-P124	Valproic acid plus hydroxyurea	6
A15-P129	Best supportive care	6
	Low risk patients, i.e. favorable genetic abnormalities	
F1-P110	Best supportive care	<1
F2-P116	Death from acute GVHD after allogeneic SCT in second CR	25
F3-P139	ATRA, valproic acid, low-dose cytarabine	<1
F4-P141	Valproic acid plus hydroxyurea	3
F5-P127	Lost from follow-up	-
F6-P131	Intensive chemotherapy followed by autologous SCT	>56
F7-P137	Azacitidine	3
F8-P144	Intensive induction and consolidation chemotherapy	>38
F9-P154	High-dose chemotherapy	>144
F10-P101	One cycle of intensive induction therapy with CR, no further chemotherapy due to severe toxicity	28
F11-P118	Intensive induction therapy with CR, toxic death during consolidation	2
F12-P120	Death from hyperleukocytosis	<1
F13-P125	Intensive induction with CR, toxic death during consolidation therapy	2
F14-P138	Intensive chemotherapy followed by autologous SCT, non-relapse death	14
F15-P143	Intensive induction with CR, toxic death during consolidation chemotherapy	2
F16-P153	AML-stabilizing therapy based on ATRA and valproic acid	2
F17-P155	Best supportive care	2
F18-P142	Intensive chemotherapy followed by autologous SCT	>44

[1]Abbreviations: ATRA, all-trans retinoic acid; CR, complete transmission; GVHD, Graft versus host disease; SCT: stem cell transplantation.

[2]The sign > means that the patient is still alive without relapse.

Supplementary Table 3. Classification of differentially expressed proteins and phosphorylated phosphoproteins found in the comparative studies between nine elderly low-risk and nine younger low-risk patients based on hallmarks of aging as explained in previous publications [1–3].

Classification	Genomic stability, DNA repair	Mitosis, cell cycle	Epigenetics, chromatin, transcription, RNA splicing, ribosome	Protein homeostasis, metabolism, protein modification	Mitochondria, metabolism	Cytoskeleton, actin polarization	Intracellular ER[1]-Golgi trafficking	Intracellular signaling	Extracellular secretion	Membrane structure	Tumor suppressor	Regulation of senescence	Regulation of apoptosis
Altered protein level in low-risk patients	APTX CAAP1 NME3 POLB	CDC27 KIAA1279 NUMB	CHD2 MARS2 MINA RPS6KA4 WARS2	ASPH BAG2 CDC27 KIAA1279 NME3 PDP1 PTPLAD2 STX7 UFSP2 NUMB	ALDH2 CLC COX6A1 KIAA1279 MARS2 NXT2 PDF PDP1 PTDSS1 WARS2	CAP1 GIT1 SKAP2	KIAA1279 NXT2 STX7	GIT1 MOB4 NENF SKAP2	NENF	PTDSS1 NUMB	PTPLAD2		CAAP1
Increased phosphorylation in elderly low-risk patients	RMI1 TOX4 TP53BP1	CBX1 HECA TMPO	ARID1A AHNAK CBX1 DDX41 IRF2BP1 KANSL1 KDM3B RERE RPS6KA4 SP100 TCEAL3 TMPO TOX4 TP53BP1 ZMYND8	DTNBP1		ARIDA1 FAM21C FNBP1L LSP1 MYO18A REPS1	BIN1 REPS1 SEC61B WDR44	DOCK5 FAM65B	LILRB3		BIN1 TP53BP1		BIN1 RERE
Decreased phosphorylation in elderly low-risk patients	LIG1	CDK1 CDK2 ESCO2 FAM83H FOXK2 GSG2 INCENP RB1	AATF ATAD2 BCLAF1 CHAF1A CHD4 CHD9 CNP EIF3F ESCO2 FOXK2 GSG2 HIST1H1D IGF2BP1 ING5 KMT2A NPM1 PPIG PRPF40A RPRD2 RRP1B RRP36 SRRM1 SRRM2	ATAD2 BCLAF1 EEF2 HSP90AB1 NPM1 POLA2 PPP6R3	CDK2 ESYT2 FOXK2 PCYT1B	IGF2BP1 SCRIB		IGF2BP1 IRS2			AATF EIF3F ING5 RB1 SCRIB	CDK2	AATF BCLAF1 FOXK2
N[2]	8	14	43	18	14	11	7	8	2	2	8	1	6

The table is based on information from the Gene database and selected references are from the PubMed database as described more in detail in Supplementary Tables 4–6.

Abbreviations: [1]ER, endoplasmic reticulum; [2]N, number of proteins.

Supplementary Table 4. Proteins with significantly altered level in low-risk patients.

Supplementary Table 5. Proteins with significantly higher phosphorylation in elderly low-risk patients.

Supplementary Table 6. Proteins with significantly lower phosphorylation in elderly low-risk patients.

Supplementary Table 7. Proteins with significantly different expression and phosphorylation levels in high-risk and low-risk patients.

Supplementary Table 8. Differentially regulated CDK1/2 phosphorylation sites identified by immunoprecipitation and LC-MS/MS analysis.

Protein	Phosphosites	FC high-risk/low-risk (LIMMA)
CDK1	T14	2.82
CDK2	T14	2.82
CDK1	T14 Y15	2.32
CDK2	T14 Y15	2.30

Phosphosites CDK1/2 T14 and Y15 were enriched using anti-pTyr-antibody immunoprecipitation and analyzed by LC-MS/MS. Significant phosphorylation differences between the high-risk and the low-risk groups were calculated with LIMMA statistics. The table below shows differentially regulated tyrosine-phosphorylated peptides with *Q*-values <0.05.

Supplementary References

1. López-Otín C, Blasco MA, Partridge L, Serrano M, Kroemer G. The hallmarks of aging. Cell. 2013; 153:1194–217. https://doi.org/10.1016/j.cell.2013.05.039 PMID:23746838

2. Lee J, Yoon SR, Choi I, Jung H. Causes and mechanisms of hematopoietic stem cell aging. Int J Mol Sci. 2019; 20:1272. https://doi.org/10.3390/ijms20061272 PMID:30871268

3. Zjablovskaja P, Florian MC. Acute myeloid leukemia: aging and epigenetics. Cancers (Basel). 2019; 12:103. https://doi.org/10.3390/cancers12010103 PMID:31906064

4. Hu XY, Fang Q, Ma D, Jiang L, Yang Y, Sun J, Yang C, Wang JS. Aldehyde dehydrogenase 2 protects human umbilical vein endothelial cells against oxidative damage and increases endothelial nitric oxide production to reverse nitroglycerin tolerance. Genet Mol Res. 2016; 15. https://doi.org/10.4238/gmr.15027822 PMID:27323160

5. Woolthuis CM, Park CY. Hematopoietic stem/ progenitor cell commitment to the megakaryocyte lineage. Blood. 2016; 127:1242–48. https://doi.org/10.1182/blood-2015-07-607945 PMID:26787736

6. Aslam MA, Alemdehy MF, Pritchard CE, Song JY, Muhaimin FI, Wijdeven RH, Huijbers IJ, Neefjes J, Jacobs H. Towards an understanding of C9orf82 protein/CAAP1 function. PLoS One. 2019; 14:e0210526. https://doi.org/10.1371/journal.pone.0210526 PMID:30629682

7. Rodríguez D, Bretones G, Quesada V, Villamor N, Arango JR, López-Guillermo A, Ramsay AJ, Baumann T, Quirós PM, Navarro A, Royo C, Martín-Subero JI, Campo E, López-Otín C. Mutations in CHD2 cause defective association with active chromatin in chronic lymphocytic leukemia. Blood. 2015; 126:195–202. https://doi.org/10.1182/blood-2014-10-604959 PMID:26031915

8. Tanna CE, Goss LB, Ludwig CG, Chen PW. Arf GAPs as regulators of the actin cytoskeleton-an update. Int J Mol Sci. 2019; 20:442. https://doi.org/10.3390/ijms20020442 PMID:30669557

9. van Gastel J, Boddaert J, Jushaj A, Premont RT, Luttrell LM, Janssens J, Martin B, Maudsley S. GIT2-a keystone in ageing and age-related disease. Ageing Res Rev. 2018; 43:46–63. https://doi.org/10.1016/j.arr.2018.02.002 PMID:29452267

10. Buschman MD, Field SJ. MYO18A: an unusual myosin. Adv Biol Regul. 2018; 67:84–92. https://doi.org/10.1016/j.jbior.2017.09.005 PMID:28942352

11. Kevenaar JT, Bianchi S, van Spronsen M, Olieric N, Lipka J, Frias CP, Mikhaylova M, Harterink M, Keijzer N, Wulf PS, Hilbert M, Kapitein LC, de Graaff E, et al. Kinesin-binding protein controls microtubule dynamics and cargo trafficking by regulating kinesin motor activity. Curr Biol. 2016; 26:849–61. https://doi.org/10.1016/j.cub.2016.01.048 PMID:26948876

12. Malaby HL, Dumas ME, Ohi R, Stumpff J. Kinesin-binding protein ensures accurate chromosome segregation by buffering KIF18A and KIF15. J Cell Biol. 2019; 218:1218–34. https://doi.org/10.1083/jcb.201806195 PMID:30709852

13. Zhang Q, Thakur C, Shi J, Sun J, Fu Y, Stemmer P, Chen F. New discoveries of mdig in the epigenetic regulation of cancers. Semin Cancer Biol. 2019; 57:27–35. https://doi.org/10.1016/j.semcancer.2019.06.013 PMID:31276784

14. Chen M, Zhang H, Shi Z, Li Y, Zhang X, Gao Z, Zhou L, Ma J, Xu Q, Guan J, Cheng Y, Jiao S, Zhou Z. The MST4-MOB4 complex disrupts the MST1-MOB1 complex in the hippo-YAP pathway and plays a pro-oncogenic role in pancreatic cancer. J Biol Chem. 2018; 293:14455–69. https://doi.org/10.1074/jbc.RA118.003279 PMID:30072378

15. Yeung YT, Guerrero-Castilla A, Cano M, Muñoz MF, Ayala A, Argüelles S. Dysregulation of the hippo pathway signaling in aging and cancer. Pharmacol Res. 2019; 143:151–65. https://doi.org/10.1016/j.phrs.2019.03.018 PMID:30910741

16. Kimura I, Konishi M, Asaki T, Furukawa N, Ukai K, Mori M, Hirasawa A, Tsujimoto G, Ohta M, Itoh N, Fujimoto M. Neudesin, an extracellular heme-binding protein, suppresses adipogenesis in 3T3-L1 cells via the MAPK cascade. Biochem Biophys Res Commun. 2009; 381:75–80. https://doi.org/10.1016/j.bbrc.2009.02.011 PMID:19351598

17. Puts GS, Leonard MK, Pamidimukkala NV, Snyder DE, Kaetzel DM. Nuclear functions of NME proteins. Lab Invest. 2018; 98:211–18. https://doi.org/10.1038/labinvest.2017.109 PMID:29058704

18. Singh KP, Bennett JA, Casado FL, Walrath JL, Welle SL, Gasiewicz TA. Loss of aryl hydrocarbon receptor promotes gene changes associated with premature hematopoietic stem cell exhaustion and development of a myeloproliferative disorder in aging mice. Stem Cells Dev. 2014; 23:95–106. https://doi.org/10.1089/scd.2013.0346 PMID:24138668

19. Stacpoole PW. The pyruvate dehydrogenase complex as a therapeutic target for age-related diseases. Aging Cell. 2012; 11:371–77. https://doi.org/10.1111/j.1474-9726.2012.00805.x PMID:22321732

20. Lillenes MS, Espeseth T, Støen M, Lundervold AJ, Frye SA, Rootwelt H, Reinvang I, Tønjum T. DNA base excision repair gene polymorphisms modulate human cognitive performance and decline during normal life span. Mech Ageing Dev. 2011; 132:449–58. https://doi.org/10.1016/j.mad.2011.08.002 PMID:21884718

21. Zhu S, Wang Z, Zhang Z, Wang J, Li Y, Yao L, Mei Q, Zhang W. PTPLAD2 is a tumor suppressor in esophageal squamous cell carcinogenesis. FEBS Lett. 2014; 588:981–89. https://doi.org/10.1016/j.febslet.2014.01.058 PMID:24530685

22. Camici GG, Savarese G, Akhmedov A, Lüscher TF. Molecular mechanism of endothelial and vascular aging: implications for cardiovascular disease. Eur Heart J. 2015; 36:3392–403. https://doi.org/10.1093/eurheartj/ehv587 PMID:26543043

23. Kopetz S, Shah AN, Gallick GE. Src continues aging: current and future clinical directions. Clin Cancer Res. 2007; 13:7232–36. https://doi.org/10.1158/1078-0432.CCR-07-1902 PMID:18094400

24. Krosl J, Mamo A, Chagraoui J, Wilhelm BT, Girard S, Louis I, Lessard J, Perreault C, Sauvageau G. A mutant allele of the Swi/Snf member BAF250a determines the pool size of fetal liver hemopoietic stem cell populations. Blood. 2010; 116:1678–84. https://doi.org/10.1182/blood-2010-03-273862 PMID:20522713

25. Ruiz-Lafuente N, Minguela A, Muro M, Parrado A. The role of DOCK10 in the regulation of the transcriptome and aging. Heliyon. 2019; 5:e01391. https://doi.org/10.1016/j.heliyon.2019.e01391 PMID:30963125

26. Watanabe R, Ui A, Kanno S, Ogiwara H, Nagase T, Kohno T, Yasui A. SWI/SNF factors required for cellular resistance to DNA damage include ARID1A and ARID1B and show interdependent protein stability. Cancer Res. 2014; 74:2465–75. https://doi.org/10.1158/0008-5472.CAN-13-3608 PMID:24788099

27. Kadono M, Kanai A, Nagamachi A, Shinriki S, Kawata J, Iwato K, Kyo T, Oshima K, Yokoyama A, Kawamura T, Nagase R, Inoue D, Kitamura T, et al. Biological implications of somatic DDX41 p.R525H mutation in acute myeloid leukemia. Exp Hematol. 2016; 44:745–54.e4. https://doi.org/10.1016/j.exphem.2016.04.017 PMID:27174803

28. Makishima H. [Sequential acquisition of mutations in myelodysplastic syndromes]. Rinsho Ketsueki. 2017; 58:1828–37. https://doi.org/10.11406/rinketsu.58.1828 PMID:28978821

29. Geiger H, Zheng Y. Cdc42 and aging of hematopoietic stem cells. Curr Opin Hematol. 2013; 20:295–300. https://doi.org/10.1097/MOH.0b013e3283615aba PMID:23615056

30. Hao YH, Doyle JM, Ramanathan S, Gomez TS, Jia D, Xu M, Chen ZJ, Billadeau DD, Rosen MK, Potts PR. Regulation of WASH-dependent actin polymerization and protein trafficking by ubiquitination. Cell. 2013; 152:1051–64. https://doi.org/10.1016/j.cell.2013.01.051 PMID:23452853

31. Singh J, Kumar S, Krishna CV, Rattan S. Aging-associated oxidative stress leads to decrease in IAS tone via RhoA/ROCK downregulation. Am J Physiol Gastrointest Liver Physiol. 2014; 306:G983–91. https://doi.org/10.1152/ajpgi.00087.2014 PMID:24742984

32. Tapia PC. RhoA, rho kinase, JAK2, and STAT3 may be the intracellular determinants of longevity implicated in the progeric influence of obesity: insulin, IGF-1, and leptin may all conspire to promote stem cell exhaustion. Med Hypotheses. 2006; 66:570–76. https://doi.org/10.1016/j.mehy.2005.09.008 PMID:16226846

33. Florian MC, Dörr K, Niebel A, Daria D, Schrezenmeier H, Rojewski M, Filippi MD, Hasenberg A, Gunzer M, Scharffetter-Kochanek K, Zheng Y, Geiger H. Cdc42 activity regulates hematopoietic stem cell aging and rejuvenation. Cell Stem Cell. 2012; 10:520–30. https://doi.org/10.1016/j.stem.2012.04.007 PMID:22560076

34. Florian MC, Klose M, Sacma M, Jablanovic J, Knudson L, Nattamai KJ, Marka G, Vollmer A, Soller K, Sakk V, Cabezas-Wallscheid N, Zheng Y, Mulaw MA, et al.

Aging alters the epigenetic asymmetry of HSC division. PLoS Biol. 2018; 16:e2003389. https://doi.org/10.1371/journal.pbio.2003389 PMID:30235201

35. Ramalho-Oliveira R, Oliveira-Vieira B, Viola JP. IRF2BP2: a new player in the regulation of cell homeostasis. J Leukoc Biol. 2019; 106:717–23. https://doi.org/10.1002/JLB.MR1218-507R PMID:31022319

36. Brauchle M, Yao Z, Arora R, Thigale S, Clay I, Inverardi B, Fletcher J, Taslimi P, Acker MG, Gerrits B, Voshol J, Bauer A, Schübeler D, et al. Protein complex interactor analysis and differential activity of KDM3 subfamily members towards H3K9 methylation. PLoS One. 2013; 8:e60549. https://doi.org/10.1371/journal.pone.0060549 PMID:23593242

37. Li J, Yu B, Deng P, Cheng Y, Yu Y, Kevork K, Ramadoss S, Ding X, Li X, Wang CY. Author correction: KDM3 epigenetically controls tumorigenic potentials of human colorectal cancer stem cells through Wnt/β-catenin signalling. Nat Commun. 2019; 10:5020. https://doi.org/10.1038/s41467-019-12878-z PMID:31685815

38. Lai WF, Wong WT. Roles of the actin cytoskeleton in aging and age-associated diseases. Ageing Res Rev. 2020; 58:101021. https://doi.org/10.1016/j.arr.2020.101021 PMID:31968269

39. Martin-Rendon E, Hale SJ, Ryan D, Baban D, Forde SP, Roubelakis M, Sweeney D, Moukayed M, Harris AL, Davies K, Watt SM. Transcriptional profiling of human cord blood CD133+ and cultured bone marrow mesenchymal stem cells in response to hypoxia. Stem Cells. 2007; 25:1003–12. https://doi.org/10.1634/stemcells.2006-0398 PMID:17185612

40. Bocquet N, Bizard AH, Abdulrahman W, Larsen NB, Faty M, Cavadini S, Bunker RD, Kowalczykowski SC, Cejka P, Hickson ID, Thomä NH. Structural and mechanistic insight into holliday-junction dissolution by topoisomerase IIIα and RMI1. Nat Struct Mol Biol. 2014; 21:261–68. https://doi.org/10.1038/nsmb.2775 PMID:24509834

41. Bounaix Morand du Puch C, Barbier E, Kraut A, Couté Y, Fuchs J, Buhot A, Livache T, Sève M, Favier A, Douki T, Gasparutto D, Sauvaigo S, Breton J. TOX4 and its binding partners recognize DNA adducts generated by platinum anticancer drugs. Arch Biochem Biophys. 2011; 507:296–303. https://doi.org/10.1016/j.abb.2010.12.021 PMID:21184731

42. Vanheer L, Song J, De Geest N, Janiszewski A, Talon I, Provenzano C, Oh T, Chappell J, Pasque V. Tox4 modulates cell fate reprogramming. J Cell Sci. 2019; 132:jcs232223. https://doi.org/10.1242/jcs.232223 PMID:31519808

43. Barbosa K, Li S, Adams PD, Deshpande AJ. The role of TP53 in acute myeloid leukemia: challenges and opportunities. Genes Chromosomes Cancer. 2019; 58:875–88. https://doi.org/10.1002/gcc.22796 PMID:31393631

44. Ou HL, Schumacher B. DNA damage responses and p53 in the aging process. Blood. 2018; 131:488–95. https://doi.org/10.1182/blood-2017-07-746396 PMID:29141944

45. Wu D, Prives C. Relevance of the p53-MDM2 axis to aging. Cell Death Differ. 2018; 25:169–79. https://doi.org/10.1038/cdd.2017.187 PMID:29192902

46. Chen J, Wang A, Chen Q. SirT3 and p53 deacetylation in aging and cancer. J Cell Physiol. 2017; 232:2308–11. https://doi.org/10.1002/jcp.25669 PMID:27791271

47. Rufini A, Tucci P, Celardo I, Melino G. Senescence and aging: the critical roles of p53. Oncogene. 2013; 32:5129–43. https://doi.org/10.1038/onc.2012.640 PMID:23416979

48. Kaiser RW, Ignarski M, Van Nostrand EL, Frese CK, Jain M, Cukoski S, Heinen H, Schaechter M, Seufert L, Bunte K, Frommolt P, Keller P, Helm M, et al. A protein-RNA interaction atlas of the ribosome biogenesis factor AATF. Sci Rep. 2019; 9:11071. https://doi.org/10.1038/s41598-019-47552-3 PMID:31363146

49. Koo SJ, Fernández-Montalván AE, Badock V, Ott CJ, Holton SJ, von Ahsen O, Toedling J, Vittori S, Bradner JE, Gorjánácz M. ATAD2 is an epigenetic reader of newly synthesized histone marks during DNA replication. Oncotarget. 2016; 7:70323–35. https://doi.org/10.18632/oncotarget.11855 PMID:27612420

50. Morozumi Y, Boussouar F, Tan M, Chaikuad A, Jamshidikia M, Colak G, He H, Nie L, Petosa C, de Dieuleveult M, Curtet S, Vitte AL, Rabatel C, et al. Atad2 is a generalist facilitator of chromatin dynamics in embryonic stem cells. J Mol Cell Biol. 2016; 8:349–62. https://doi.org/10.1093/jmcb/mjv060 PMID:26459632

51. Shao AW, Sun H, Geng Y, Peng Q, Wang P, Chen J, Xiong T, Cao R, Tang J. Bclaf1 is an important NF-κB signaling transducer and C/EBPβ regulator in DNA damage-induced senescence. Cell Death Differ. 2016; 23:865–75. https://doi.org/10.1038/cdd.2015.150 PMID:26794446

52. Chae U, Park JW, Lee SR, Lee HJ, Lee HS, Lee DS. Reactive oxygen species-mediated senescence is accelerated by inhibiting Cdk2 in Idh2-deficient conditions. Aging (Albany NY). 2019; 11:7242–56. https://doi.org/10.18632/aging.102259 PMID:31503005

53. Heshmati Y, Türköz G, Harisankar A, Kharazi S, Boström J, Dolatabadi EK, Krstic A, Chang D, Månsson R, Altun M, Qian H, Walfridsson J. The chromatin-remodeling factor CHD4 is required for maintenance of childhood acute myeloid leukemia. Haematologica. 2018; 103:1169–81. https://doi.org/10.3324/haematol.2017.183970 PMID:29599201

54. Sperlazza J, Rahmani M, Beckta J, Aust M, Hawkins E, Wang SZ, Zu Zhu S, Podder S, Dumur C, Archer K, Grant S, Ginder GD. Depletion of the chromatin remodeler CHD4 sensitizes AML blasts to genotoxic agents and reduces tumor formation. Blood. 2015; 126:1462–72. https://doi.org/10.1182/blood-2015-03-631606 PMID:26265695

55. Ooga M, Funaya S, Hashioka Y, Fujii W, Naito K, Suzuki MG, Aoki F. Chd9 mediates highly loosened chromatin structure in growing mouse oocytes. Biochem Biophys Res Commun. 2018; 500:583–88. https://doi.org/10.1016/j.bbrc.2018.04.105 PMID:29665362

56. Unlu I, Lu Y, Wang X. The cyclic phosphodiesterase CNP and RNA cyclase RtcA fine-tune noncanonical XBP1 splicing during ER stress. J Biol Chem. 2018; 293:19365–76. https://doi.org/10.1074/jbc.RA118.004872 PMID:30355738

57. Xie J, de Souza Alves V, von der Haar T, O'Keefe L, Lenchine RV, Jensen KB, Liu R, Coldwell MJ, Wang X, Proud CG. Regulation of the elongation phase of protein synthesis enhances translation accuracy and modulates lifespan. Curr Biol. 2019; 29:737–49.e5. https://doi.org/10.1016/j.cub.2019.01.029 PMID:30773367

58. Wen F, Zhou R, Shen A, Choi A, Uribe D, Shi J. The tumor suppressive role of eIF3f and its function in translation inhibition and rRNA degradation. PLoS One. 2012; 7:e34194. https://doi.org/10.1371/journal.pone.0034194 PMID:22457825

59. Schauder CM, Wu X, Saheki Y, Narayanaswamy P, Torta F, Wenk MR, De Camilli P, Reinisch KM. Structure of a lipid-bound extended synaptotagmin indicates a role in lipid transfer. Nature. 2014; 510:552–55. https://doi.org/10.1038/nature13269 PMID:24847877

60. Yang Q, Wang J, Zhong P, Mou T, Hua H, Liu P, Xie F. The clinical prognostic value of lncRNA FAM83H-AS1 in cancer patients: a meta-analysis. Cancer Cell Int. 2020; 20:72. https://doi.org/10.1186/s12935-020-1148-8 PMID:32165862

61. Lin MF, Yang YF, Peng ZP, Zhang MF, Liang JY, Chen W, Liu XH, Zheng YL. FOXK2, regulted by miR-1271-5p, promotes cell growth and indicates unfavorable prognosis in hepatocellular carcinoma. Int J Biochem Cell Biol. 2017; 88:155–61. https://doi.org/10.1016/j.biocel.2017.05.019 PMID:28506857

62. Liu X, Wei X, Niu W, Wang D, Wang B, Zhuang H. Downregulation of FOXK2 is associated with poor prognosis in patients with gastric cancer. Mol Med Rep. 2018; 18:4356–64. https://doi.org/10.3892/mmr.2018.9466 PMID:30221666

63. Nestal de Moraes G, Carneiro LD, Maia RC, Lam EW, Sharrocks AD. FOXK2 transcription factor and its emerging roles in cancer. Cancers (Basel). 2019; 11:393. https://doi.org/10.3390/cancers11030393 PMID:30897782

64. Balboula AZ, Nguyen AL, Gentilello AS, Quartuccio SM, Drutovic D, Solc P, Schindler K. Haspin kinase regulates microtubule-organizing center clustering and stability through aurora kinase C in mouse oocytes. J Cell Sci. 2016; 129:3648–60. https://doi.org/10.1242/jcs.189340 PMID:27562071

65. Liang C, Chen Q, Yi Q, Zhang M, Yan H, Zhang B, Zhou L, Zhang Z, Qi F, Ye S, Wang F. A kinase-dependent role for haspin in antagonizing wapl and protecting mitotic centromere cohesion. EMBO Rep. 2018; 19:43–56. https://doi.org/10.15252/embr.201744737 PMID:29138236

66. Maiolica A, de Medina-Redondo M, Schoof EM, Chaikuad A, Villa F, Gatti M, Jeganathan S, Lou HJ, Novy K, Hauri S, Toprak UH, Herzog F, Meraldi P, et al. Modulation of the chromatin phosphoproteome by the haspin protein kinase. Mol Cell Proteomics. 2014; 13:1724–40. https://doi.org/10.1074/mcp.M113.034819 PMID:24732914

67. Short B. GTSE1 leads cancer cells into CIN. J Cell Biol. 2016; 215:593. https://doi.org/10.1083/jcb.2155if PMID:27888203

68. Thalappilly S, Feng X, Pastyryeva S, Suzuki K, Muruve D, Larocque D, Richard S, Truss M, von Deimling A, Riabowol K, Tallen G. The p53 tumor suppressor is

stabilized by inhibitor of growth 1 (ING1) by blocking polyubiquitination. PLoS One. 2011; 6:e21065. https://doi.org/10.1371/journal.pone.0021065 PMID:21731648

69. Schmidt K, Zhang Q, Tasdogan A, Petzold A, Dahl A, Arneth BM, Slany R, Fehling HJ, Kranz A, Stewart AF, Anastassiadis K. The H3K4 methyltransferase Setd1b is essential for hematopoietic stem and progenitor cell homeostasis in mice. Elife. 2018; 7:e27157. https://doi.org/10.7554/eLife.27157 PMID:29916805

70. Cornell RB, Ridgway ND. CTP:phosphocholine cytidylyltransferase: function, regulation, and structure of an amphitropic enzyme required for membrane biogenesis. Prog Lipid Res. 2015; 59:147–71. https://doi.org/10.1016/j.plipres.2015.07.001 PMID:26165797

71. Ganduri S, Lue NF. STN1-POLA2 interaction provides a basis for primase-pol α stimulation by human STN1. Nucleic Acids Res. 2017; 45:9455–66. https://doi.org/10.1093/nar/gkx621 PMID:28934486

72. Szlavicz E, Szabo K, Groma G, Bata-Csorgo Z, Pagani F, Kemeny L, Szell M. Splicing factors differentially expressed in psoriasis alter mRNA maturation of disease-associated EDA+ fibronectin. Mol Cell Biochem. 2017; 436:189–99. https://doi.org/10.1007/s11010-017-3090-1 PMID:28589370

73. Qiu R, Zhang J, Xiang X. The splicing-factor Prp40 affects dynein-dynactin function in Aspergillus nidulans. Mol Biol Cell. 2020; 31:1289–301. https://doi.org/10.1091/mbc.E20-03-0166 PMID:32267207

74. Ni Z, Xu C, Guo X, Hunter GO, Kuznetsova OV, Tempel W, Marcon E, Zhong G, Guo H, Kuo WW, Li J, Young P, Olsen JB, et al. RPRD1A and RPRD1B are human RNA polymerase II C-terminal domain scaffolds for Ser5 dephosphorylation. Nat Struct Mol Biol. 2014; 21:686–95. https://doi.org/10.1038/nsmb.2853 PMID:24997600

75. Alsarraj J, Faraji F, Geiger TR, Mattaini KR, Williams M, Wu J, Ha NH, Merlino T, Walker RC, Bosley AD, Xiao Z, Andresson T, Esposito D, et al. BRD4 short isoform interacts with RRP1B, SIPA1 and components of the LINC complex at the inner face of the nuclear membrane. PLoS One. 2013; 8:e80746. https://doi.org/10.1371/journal.pone.0080746 PMID:24260471

76. Lee M, Dworkin AM, Gildea D, Trivedi NS, Moorhead GB, Crawford NP, and NISC Comparative Sequencing Program. RRP1B is a metastasis modifier that regulates the expression of alternative mRNA isoforms through interactions with SRSF1. Oncogene. 2014; 33:1818–27. https://doi.org/10.1038/onc.2013.133 PMID:23604122

77. Maiese K. Disease onset and aging in the world of circular RNAs. J Transl Sci. 2016; 2:327–29. https://doi.org/10.15761/jts.1000158 PMID:27642518

78. Gérus M, Bonnart C, Caizergues-Ferrer M, Henry Y, Henras AK. Evolutionarily conserved function of RRP36 in early cleavages of the pre-rRNA and production of the 40S ribosomal subunit. Mol Cell Biol. 2010; 30:1130–44. https://doi.org/10.1128/MCB.00999-09 PMID:20038530

79. Dash BP, Schnöder TM, Kathner C, Mohr J, Weinert S, Herzog C, Godavarthy PS, Zanetti C, Perner F, Braun-Dullaeus R, Hartleben B, Huber TB, Walz G, et al. Diverging impact of cell fate determinants scrib and Llgl1 on adhesion and migration of hematopoietic stem cells. J Cancer Res Clin Oncol. 2018; 144:1933–44. https://doi.org/10.1007/s00432-018-2724-3 PMID:30083817

80. Chwalenia K, Qin F, Singh S, Li H. A cell-based splicing reporter system to identify regulators of cis-splicing between adjacent genes. Nucleic Acids Res. 2019; 47:e24. https://doi.org/10.1093/nar/gky1288 PMID:30590765

81. Zanini IM, Soneson C, Lorenzi LE, Azzalin CM. Human cactin interacts with DHX8 and SRRM2 to assure efficient pre-mRNA splicing and sister chromatid cohesion. J Cell Sci. 2017; 130:767–78. https://doi.org/10.1242/jcs.194068 PMID:28062851

82. Bhullar J, Sollars VE. YBX1 expression and function in early hematopoiesis and leukemic cells. Immunogenetics. 2011; 63:337–50. https://doi.org/10.1007/s00251-011-0517-9 PMID:21369783

83. Knuckles P, Lence T, Haussmann IU, Jacob D, Kreim N, Carl SH, Masiello I, Hares T, Villaseñor R, Hess D, Andrade-Navarro MA, Biggiogera M, Helm M, et al. Zc3h13/flacc is required for adenosine methylation by bridging the mRNA-binding factor Rbm15/Spenito to the m^6A machinery component Wtap/Fl(2)d. Genes Dev. 2018; 32:415–29. https://doi.org/10.1101/gad.309146.117 PMID:29535189

84. Wen J, Lv R, Ma H, Shen H, He C, Wang J, Jiao F, Liu H, Yang P, Tan L, Lan F, Shi YG, He C, et al. Zc3h13 regulates nuclear RNA m^6A methylation and mouse embryonic stem cell self-renewal. Mol Cell. 2018; 69:1028–38.e6. https://doi.org/10.1016/j.molcel.2018.02.015 PMID:29547716

Supplementary Files

Please browse Full Text version to see the data of Supplementary Files 1–5.

Supplementary File 1. Proteomic quantification of 18 low-risk patients.

Supplementary File 2. Phosphoproteomic quantification of 18 low-risk patients.

Supplementary File 3. Proteomic quantification of 15 high-risk and 18 low-risk patients.

Supplementary File 4. Phosphoproteomic quantification of 15 high-risk and 18 low-risk patients.

Supplementary File 5. pTyr_Phosphoproteomic quantification of 5 high-risk and 6 low-risk patients.

Supplementary Data Analysis

Supplementary Analysis

The proliferative *in vitro* responsiveness of primary human AML cells derived from 63 consecutive patients.

The proliferative responsiveness was tested by a [^{3}H]-thymidine incorporation assay prepared in serum-free medium as described in a previous article [1]. All growth factors were tested at a final concentration of 20 ng/ml. During *in vitro* culture AML cells undergo spontaneous apoptosis. We tested [^{3}H]-thymidine by adding [^{3}H]-thymidine after six days of culture, and the cultures were harvested 24 hours later. Thus, the proliferative responsiveness reflects the characteristics for a subset of cells within the hierarchically organized AML cell population that is capable of surviving for at least six days and still be able to show detectable proliferation.

The results are presented as number of patients with detectable proliferation, this was defined as a [^{3}H]-thymidine incorporation corresponding to >1000 cpm. Patient characteristics are described in the first table

Supplementary Reference

1. Bruserud Ø, Ryningen A, Olsnes AM, Stordrange L, Øyan AM, Kalland KH, Gjertsen BT. Subclassification of patients with acute myelogenous leukemia based on chemokine responsiveness and constitutive chemokine release by their leukemic cells. Haematologica. 2007; 92:332–41.
https://doi.org/10.3324/haematol.10148
PMID:17339182

Supplementary Analysis Table 1. Characteristics of 63 consecutive patients used in the study of possible associations between age and differentiation.

Younger patients (<65 years of age, n=38)				**Elderly patients (>65 years of age, n=25)**			
Male/female 20/18		*Karyotype*		Male/female 15/10		*Karyotype*	
		Favorable	2			Favorable	1
FAB classification		Adverse	4	*FAB classification*		Adverse	4
M0	3	Intermediate	10	M0	5	Intermediate	2
M1	6	Normal	18	M1	5	Normal	3
M2	10	Not tested	4	M2	7	Not tested	15
M4	**11**			**M4**	**5**		
M5	**7**	*FLT3 abnormalities*		**M5**	**3**	*FLT3 abnormalities*	
M6	1	ITD	11	M6	0	ITD	8
		D835	2			D835	2
		WT	18			WT	12
		Not tested	7			Not tested	3
CD34 expression	18			*CD34 expression*	11		
de novo	31			*de novo*	16		
Predisposition		*NPM1 abnormalities*		*Predisposition*		*NPM1 abnormalities*	
MDS	1	Insertion	8	MDS	6	Insertion	2
MPN	1	WT	14	MPN	1	WT	20
Chemotherapy	5	Not tested	16	Chemotherapy	2	Not tested	3

COMMENTS: We investigated 63 consecutive patients with high peripheral blood blast counts (REK 1759/2015, REK 305/2017). Enriched AML cells could thereby be prepared by density gradient separation alone (see Material and methods in the main text). CD34 positivity was defined as at least 20% positive cells in flow cytometric analysis compared with the negative isotype control. The data above are presented as the number of patients. Red font indicates statistical difference between the two age groups.

In contrast to our main patient cohort that included only high- and low-risk patients, this second cohort included consecutive patients (and thereby unselected) patients and also patients with intermediate prognosis, i.e. normal or intermediate karyotype that constitutes approximately 60% of all patients in our biobank.

Supplementary Analysis Table 2. Proliferative responsiveness of the AML cells from 63 patients.

Younger patients (<65 years of age, n=38)		**Elderly patients (>65 years of age, n=25)**	
Culture condition	*Number of responders*	*Culture condition*	*Number of responders*
Medium alone	15	Medium alone	7
IL1β	27	IL1β	16
IL3	28	IL3	20
SCF	27	SCF	19
FLT3-ligand	24	FLT3-ligand	15
GM-CSF	27	GM-CSF	20
G-CSF	25	G-CSF	20
M-CSF	17	M-CSF	12
Thrombopoietin	15	Thrombopoietin	12
Patients without morphological signs of monocytic differentiation (n=36)		**Patients with morphological signs of monocytic differentiation (FAB-M4/M5, n=27)**	
Culture condition	*Number of responders*	*Culture condition*	*Number of responders*
Medium alone	14	Medium alone	8
IL1β	24	IL1β	16
IL3	30	IL3	18
SCF	29	SCF	17
FLT3-ligand	27	FLT3-ligand	12
GM-CSF	29	GM-CSF	18
G-CSF	29	G-CSF	16
M-CSF	16	M-CSF	13
Thrombopoietin	16	Thrombopoietin	11

COMMENTS: In this analysis we compared morphology, CD34 expression and proliferative responsiveness in the presence of several growth factors for a group of consecutive patients. It can be seen from Supplementary Table 1 and Table 1 that morphological signs of monocytic differentiation (i.e. FAB M4/M5) were more common among low-risk (i.e. relatively young) than among high-risk patients (Fisher's exact test, *P*= 0.039). We therefore investigated whether there were any significant associations between age (i.e. comparing patients above and below 65 years of age) and differentiation in an additional cohort that included 63 consecutive/unselected AML patients. None of the patients from the high-/low-risk groups (see Supplementary Table 1) was included among these 63 patients. Morphological signs of monocytic differentiation were significantly more frequent among younger patients also in this cohort (Fisher's exact test, *P*= 0.0334). However, patient age showed no significant associations with expression of the CD34 stem cell marker, molecular differentiation markers (i.e. CD13, CD14, CD15, CD33; data not shown) or the proliferative responsiveness to hematopoietic growth factors with (G-CSF, M-CSF, thrombopoietin) or without (IL1β, IL3, SCF, FLT3-ligand) lineage associations. The proliferative responsiveness of patients with and without morphological signs of differentiation did not differ significantly either.

CONCLUSION: Although we observed a difference in the expression of mitosis/proliferation regulatory proteins when comparing high-risk and low-risk AML patients, we could not find any evidence for a general association between differentiation status and proliferative capacity of primary human AML cells when investigating this consecutive group of patients.

Abbreviations: FAB, French-American-British; G/GM/M-CSF, granulocyte/granulocyte-monocyte/monocyte colony-stimulating factor; IL, interleukin; ITD, internal tandem duplication; MDS, myelodysplastic syndrome; MPN, myeloproliferative neoplasia; SCF, stem cell factor: WT, wild –type.